DEPARTAMENTO DE CIÊNCIAS DA VIDA

FACULDADE DE CIÊNCIAS E TECNOLOGIA
UNIVERSIDADE DE COIMBRA

Quantifying triglyceride futile cycling with deuterated water and ^{2}H NMR analysis of Glycerol ^{2}H enrichment

Cátia Marques

2015

Cátia Marília Marques Santos

Quantifying triglyceride futile cycling with deuterated water and ^{2}H NMR analysis of Glycerol ^{2}H enrichment

Dissertação apresentada para provas de Mestrado em Bioquímica na área de Metabolismo, orientada pelo Dr. John G. Jones e Dr. Ângelo Tomé, apresentada à Faculdade de Ciências e Tecnologia da Universidade de Coimbra

Julho de 2015

· U C ·

UNIVERSIDADE DE COIMBRA

“The only way to be truly satisfied

is to do what you believe is great work.

And the only way to do great work

is to love what you do.”

Steve Jobs

Acknowledgements / Agradecimentos

During my academic life different people were significant for me, from professors and colleagues to family and friends. Some were already part of my life and others were new to it, but all of them had, in different ways, a key role to my progress.

It would not be fair to neglect one teacher that I had in High School, Manuela Coelho. I am truly grateful for the support, the knowledge and for everything that she did for me.

During my graduation in Chemistry, there were different teachers that I liked but PhD. Dina Murtinho deserves a big thank you for everything that she taught me about Organic Chemistry and for being always available when I need some advice or clarification.

To my supervisor of this master dissertation, PhD. John Jones, my giant gratitude for the patience and guidance throughout everything that he has taught me during this year. But most importantly, I am grateful to him for letting me develop this dissertation under his supervision.

I am also grateful to PhD. Ângelo Tomé, for accepting to be my co-supervisor to this Master dissertation.

Thank you to the laboratory group, Filipa, Cristina, Ivan, João Rito, João Silva and Margarida, for all the help and companionship during this year. It has been a fantastic experience working with them.

A special thank you to Carmo and António for putting up with me and my bad humour from time to time, especially during the writing of this dissertation, and helping me when I needed it the most. I am also very grateful for their friendship.

Obrigada Mónica por me aturares, por estares disponível quando eu precisei, por toda a amizade e carinho, e por me ajudares a distrair quando andava mais stressada.

Mãe, obrigada por todos os esforços que fizeste ao longo dos anos. Sem estes, eu não poderia ter chegado aqui. Obrigada pelo amor e pela compreensão que sempre tiveste. Obrigada, acima de tudo, por acreditares sempre em mim e no que sou capaz. És a melhor mãe do mundo.

Mana, obrigada por me irritares, por seres chata e por seres uma das pessoas que mais me apoiou e deu força. És a melhor irmã que eu podia ter.

Avós, Aline e Eduardo, um especial obrigada por me ajudarem desde sempre, por me proporcionarem tudo o que puderam, por serem os melhores avós do mundo e por todo o amor que me deram.

Contents

List of abbreviations

^{1H}	Hidrogen
NEFA	non-esterified fatty acids
TG	Triglycerides
WAT	White adipose tissue
NTS	Non-shivering thermogenesis
UCP1	Uncoupling protein 1
FA	Fatty acids
LPL	Lipoprotein lipase
ACS	Acyl-CoA synthetase
ATP	Adenosine triphosphate
G3P	glycerol-3-phosphate
GPAT	glycerol-3-phosphate acyl transferase
AGPAT	acylglycerolphosphate acyltransferase
DGAT	diacylglycerol acyltransferase
CL	ATP-citrate lyase
ACC	acetyl-CoA carboxylase
FAZ	fatty acid synthase
SCD1	Δ-9 desaturase-stearoyl-CoA desaturase
GK	glycerol kinase
DHAP	dihydroxyacetone phosphate
PC	pyruvate carboxylase
PEP	phosphoenolpyruvate
PEPCK	phosphoenolpyruvate carboxylase

PDH	pyruvate dehydrogenase
ATGL	adipose triglyceride lipase
HSL	hormone-sensitive lipase
MGL	monoglyceride lipase
CPT1	carnitine palmitoyltransferase 1
NADH	Nicotineamide adenine dinucleotide
FADH2	Flavin adenine nucleotide
GLUT4	glucose transporter 4
ACAD	acyl-CoA dehydrogenases
VLCAD	very long chain ACAD
LCAD	long chain ACAD
MCAD	medium chain ACAD
D2O /2H2O	deuterated water
RF	radiofrequency
FID	free-induction decay
NMR	nuclear Magnetic resonance
FT	Fourier transform
B0	magnetic field
ppm	parts per million
2H-NMR	deuterium nuclear Magnetic resonance

Summary

"Futile cycling" between triglyceride and fatty acids has been proposed as a mechanism for energy dissipation in living organisms. Our laboratory has developed a method for quantifying this rate of cycling using deuterated water ($^{2}H_2O$) to label triglycerides. This method was based on the analysis of ^{2}H-enrichment in the glyceride moiety by ^{2}H NMR. The main goal of this Master dissertation was to develop an improved method for analysing ^{2}H-enrichment in this site, since with existing triglyceride analysis, the glyceride ^{2}H NMR signals are very broad and difficult to quantify due to their restricted motion. We therefore developed protocols to quantitatively transesterify triglycerides yielding free glycerol, whose ^{2}H NMR signals are narrower and better resolved compared to those of the intact triglyceride. Since the glycerol ^{2}H NMR analysis was performed in water, we tested hexafluoroacetone, an alternative fluorine lock compound to the hexafluorobenzene currently in use –but which is not water soluble.

We applied this analysis to quantify triglyceride/fatty acid futile cycling in adipose tissue of two mice strains (AJ mice - models of obesity-resistant- and B6 mice - models of obesity-prone animals) that were exposed to 7 days of cold in order to stimulate adipocyte futile cycling and heat generation pathways.

Following optimization of the transesterification protocol, we were able to obtain average glycerol yields of 80% that of the starting triglyceride material indicating that this approach was suitable for preservation of sample mass for effective NMR analysis. The ^{2}H NMR spectrum of triglycerides shows two different peaks, one corresponds to the deuterium labelling in the carbon 2 of glyceride moiety and the other represents deuterium labelling in carbons 1 and 3 of the same moiety. The linewidths at half height for each peak are 19,46 Hz and 14,23 Hz, respectively. After the transesterification process, the ^{2}H NMR spectrum of isolated glycerol shows 3 distinct peaks, one still corresponds to the deuterium labelling in the carbon 2 and two others corresponding to the prochiral *R* and *S* hydrogens bound to carbons 1 and 3. In this analysis, the linewidths at half height are 3,41 Hz, 3,68 Hz and 3,85 Hz, respectively. These

narrower ^{2}H NMR signals resulted in more precise measurements of triglyceride glyceryl ^{2}H enrichment.

For the AJ strain, the fractional turnover rate of triglyceride glycerol, expressed in percent, were 3,24 ± 0,88% and 16,62 ± 2,63% for the control and 7 days cold exposure, respectively. For the B6 strain fractional turnover rates of 3,63 ± 1,38% and 10,03 ± 2,29% were obtained for control and 7 days cold exposure, respectively. Thus, AJ mice had significantly higher triglyceride turnover at 7 days cold exposure compared to B6 ($P < 0,0001$). This may be related to the reduced metabolic efficiency of AJ versus B6 mice that in turn may better protect the AJ strain against diet-induced obesity.

Keywords: transesterification, triglyceride futile cycling, ^{2}H NMR.

Resumo

O “Ciclo Fútil” entre triglicerídeos e ácidos gordos tem sido proposto como um mecanismo de dissipação de energia em organismos vivos. O nosso laboratório desenvolveu um método que permite a quantificação do fluxo deste ciclo utilizando água deuterada ($^{2}H_2O$) para marcar triglicerídeos. Este método baseia-se na análise do enriquecimento com deutério da fracção do glicerídeo através de ^{2}H RMN. O principal objectivo desta dissertação de mestrado era desenvolver um método melhorado para a análise do enriquecimento de ^{2}H no local já referido, uma vez que, com a análise de triglicerídeos já existente, os sinais do espectro de ^{2}H-RMN correspondentes à marcação do glicerídeos são muito largos e difíceis de quantificar devido à sua restrição de movimento. Com o intuito de melhorar a quantificação destes sinais, desenvolvemos protocolos que permitem uma transesterificação dos triglicerídeos com rendimentos elevados obtendo o glicerol isolado, cujos sinais de ^{2}H-RMN são mais estreitos e têm uma melhor resolução quando comparados com os sinais equivalentes na molécula de triglicerídeos inicial. Tendo em conta que a análise de ^{2}H-RMN do glicerol foi feita em água, nós testámos a hexafluoroacetona visto que é um composto de flúor alternativo ao hexafluorobenzeno – composto não solúvel em água.

Nós aplicámos este método para quantificar o ciclo fútil de triglicerídeos/ácidos gordos em tecido adiposo de duas estirpes diferentes de ratos (ratos AJ – modelo de resistência à obesidade – e ratos B6 – modelo com tendência à obesidade) expostos a temperaturas baixas durante 7 dias com o objectivo de estimular o ciclo fútil referido no tecido adiposo e os mecanismos de produção de calor.

Com a optimização do protocolo de transesterificação, os rendimentos médios de extracção do glicerol foram de 80% comparando com a quantidade inicial de triglicerídeos. Tal indica que esta abordagem permite a preservação da quantidade de amostra para análise por RMN. Os espectros de ^{2}H RMN dos triglicerídeos mostram a existência de dois picos, um corresponde à marcação de deutério na posição do carbono 2 da fracção do glicerídeos e o outro representa a marcação de deutério nos carbonos das posições 1 e 3 da fracção

em estudo. As larguras dos sinais a uma altura média, para cada pico, são 19,46 Hz e 14,23 Hz, respectivamente. Após a transesterificação, os espectros de ^{2}H RMN correspondentes ao glicerol isolado apresentam três picos distintos, um corresponde à marcação com deutério no carbono 2 e os outros dois correspondem aos hidrogénios proquirais *R* e *S* ligados aos carbonos 1 e 3. Nesta análise, as larguras dos sinais a média altura são 3,41 Hz, 3,68 Hz e 3,85 Hz, respectivamente. Estes sinais são mais estreitos e resultam numa quantificação mais precisa do enriquecimento da porção do glicerídeo dos triglicerídeos.

Para a estirpe AJ, a taxa de marcação da porção do glicerídeo dos triglicerídeos foi 3,24 ± 0,88% e 16,62 ± 2,63% para o grupo controlo e para o grupo exposto a temperaturas baixas durante 7 dias, respectivamente. A taxa de marcação para a estirpe B6 foi de 3,63 ± 1,38% e 10,03 ± 2,29%, respectivamente para os mesmos grupos. No entanto, para os grupos expostos a temperaturas baixas durante 7 dias, a estirpe AJ teve uma taxa de marcação significativamente maior comparando com a estirpe B6 ($P < 0,0001$). Isto pode estar relacionado com a menor eficiência metabólica da estirpe AJ versus estirpe B6, que por sua vez protege a estirpe AJ contra obesidade induzida pela dieta.

Palavras-chave: transesterificação, ciclo fútil dos triglicerídeos, ^{2}H RMN.

1. Introduction

According to the World Health Organization (WHO) overweight and obesity are defined as an “abnormal or excessive fat accumulation that presents a risk to health”. Obesity is a leading risk factor for the development of cardiovascular disease, fatty liver disease and Type 2 diabetes [1].Demographic studies show that in the last decades the number of obese and overweight people has been increasing significantly. Statistics indicate that insufficient physical activity combined with high calorie intake per day result in a higher prevalence of overweight. It is also important to highlight that countries more economically developed, such as USA, United Kingdom and Australia, are the ones with the largest frequency of overweight/obese subjects. This may be in part explained by the easy availability of so-called “fast food” ” that is high in saturated fat and sugar and the stressed life which leads to a diminution of the time left to prepare healthy meals. In addition to these environmental factors, the tendency for developing obesity may also depend on inherent characteristics [2]. For most of human history, food has been scarce and infrequent therefore the efficient storage of food as fat during times of plenty was a strong survival trait. However, these same characteristics in the present day, where food is always easily available, promote the development of obesity. As a corollary, a reduced metabolic efficiency protects against the development of obesity in this setting. The background of this work is the study of fatty acid-triglyceride futile cycling: a process that consumes energy while not contributing to any net change in lipid levels leading to a decrease in metabolic efficiency. Understanding the extent of its activity and the basis of its regulation could provide a novel paradigm for the prevention and treatment of obesity.

1.1 Lipids

Lipids have three main nutritional and metabolic roles in the organism. Primarily, they act as the principal fuel source for most tissues in the human body, including the heart, liver and skeletal muscle. Secondly, lipids represent the main form of nutrient storage in the organism and this storage capability is apparently unlimited. Thirdly, lipids are a major component of thermal control is

warm-blooded organisms since they provide insulation against cold environments and also because they are the principal substrate used for thermogenesis.

Lipids can be derived from diet and can also be synthesized in a process called *de novo lipogenesis* using other nutrients available in the organism such as carbohydrates. This process occurs mainly in the liver and it is typically tightly regulated. Newly synthesized lipids are exported from the liver as very low density lipoproteins (VLDL) and are taken up by peripheral tissues. The main recipient of lipids are adipocytes, which function as lipid storage depots but also secrete an array of hormones that contribute to whole body fuel homeostasis.

When the organism is fasting and needs substrates for oxidation and energy production, triglycerides stored in the adipocytes undergo lipolysis to obtain fatty acids and glycerol. Free-fatty acids are released into the bloodstream and are transported to target tissues via binding to albumin. Glycerol is taken up by the liver and converted to glucose.

1.2 Adipose tissue

An adipocyte is a type of connective tissue cell that has differentiated and become specialized in the synthesis and storage of lipids. These cells play a role in maintaining proper energy balance, storing calories in the form of lipids, and mobilizing energy sources in response to hormonal stimulation [1]. More recently, adipocytes have also been shown to act as endocrine tissues, secreting a diversity of hormones that modulate the functions and actions of other organs. When the adipocyte capacity to store lipids is exceeded, lipids will overflow into other tissues as liver and muscle. This so-called ectopic lipid is implicated in the development of insulin resistance and Type 2 Diabetes [1].

There exist three different kinds of adipocytes considering their morphology and function: white adipose tissue (WAT) with unilocular adipocytes, brown adipose tissue (BAT) with multilocular adipocytes and brite

adipose tissues depots. This third example is considered to be an intermediate between WAT and BAT [3].

WAT are cells characterized by one big lipid droplet and small amounts of mitochondria. Their main purpose is to store and release lipids when the organism needs them, hence the turnover between fatty acids and triglyceride that occurs inside of these cells is relatively small. WAT are also active in the endocrine regulation of other tissues and organs [1]. WAT are distributed in numerous depots but these sites can be divided in visceral – located in the trunk cavity around the intestines and liver- and subcutaneous – under the skin. The terminology used to identify individual depots depends on their location and it can differ among authors. On this dissertation we used perigonadal WAT, more precisely epididymal WAT (eWAT) since we used male animals [4].WAT present in different depots have differences on their response to hormones, endocrine function and “browning” potential. To explain these differences we can also have in account the presence of other cells, such as leukocytes, and the various origins that WAT may have [3].

BAT are characterized by multiple small lipid droplets, also called loculi, and the number of mitochondria present is significantly higher in comparison to WAT, conferring a brownish colour to the tissue. BAT has a higher metabolic rate than WAT and the main use of this energy expenditure is for non-shivering thermogenesis (NST) [5].The morphology of BAT ensures fast and efficient lipid oxidation in mitochondria thereby generating reducing equivalents for thermogenesis. Uncoupling protein 1 (UCP1), is a specific proton transporter that that is present in the inner mitochondrial membrane that enables the thermogenesis process [6].

During cold stress, NST is combined with shivering of skeletal muscles to maintain body temperature. When exposed to a chronically cold environment, BAT is recruited and a whole group of processes occur in order to maintain body temperature homeostasis. However, if the cold exposure is acute it will activate thermogenesis of pre-existing BAT thereby triggering mobilization of stored triglyceride as well as uptake of FA and glucose from blood [6]. In the

setting of thermoneutral temperatures where there is less need for heat generation, BAT undergoes atrophy.

BAT is distributed in different regions of rodents, with the largest concentration in the interscapular region and along the cervical spine [4]. Whereas in humans, it was long thought that BAT was only present in new-borns, recent positron emission tomography studies have revealed the presence of functional BAT in adult humans exposed to cold temperatures [7].

"Brite" adipose tissue depots, also called "beige" or "inducible brown", are WAT that show multilocular UCP1-positive adipocytes after adrenergic stimulation, including exposure to cold temperature [8].The process of recruitment of this "brite" adipose tissue is known as "browning" of WAT. If these adipocytes are not in a stimulated state they cannot be distinguished from classical WAT and during this state their main function is to store triglyceride. It is not clear yet what happens after stimulation but some studies indicate that these "brite" adipocytes can return to their original state [9].Thus, "brite" adipocytes are WAT that when exposed to a certain stimuli can behave like BAT, showing the same thermogenic function. WAT depots may have different origins and functions so it is possible to assume that this "browning" capability is also associated to different depots [10].

Figure 1.1 represents the morphology of each type of the adipose tissue. It is a representation of the expected size and quantity of the constituents.

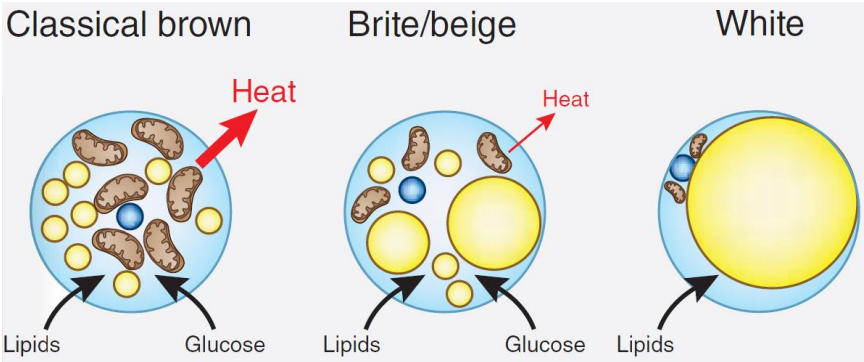

Figure 1.1 – Types of adipose tissue. The yellow circles are lipid droplets, the blue circle is the nucleus and the brown shapes are mitochondria. Adapted from reference [11].

In the beginning of this chapter it was mentioned that it is important to develop new strategies/treatments that can help to fight obesity and its co-morbidities. The capability of BAT to generate and dissipate heat through the consumption of lipids and glucose already stored has caught the attention of researchers. With the discovery of BAT in adult humans and the existence of WAT "browning" some hopes have been raised to use adipose tissue metabolism in modulation of whole body energy balance.

The energy homeostasis of the whole body has two main components: energy intake from ingested food and energy expenditure. The ingested food can be divided in two ratios, 10% of it is not absorbed by the organism and it is excreted in the form of sweat, faeces and urine [12]. The remaining 90% is used to cover energetic requirements such as tissue production and repair, temperature homeostasis and physical activities. The biggest contribution from adipose tissue to energy expenditure is thermogenesis. The main function of WAT is to store energy; hence these tissues are metabolically less active compared to BAT. With the "browning" of WAT, its overall metabolic rate is thought to increase level despite the relatively low number of brite cells.

1.3 Metabolic pathways in adipocytes: Glycolysis, Lipolysis, Glyceroneogenesis, Fatty acid esterification, *de novo* Lipogenesis and *β-Oxidation*

Adipose tissue has the primary function of storing triglycerides (TG) in the form of lipid droplets. After feeding, high levels of triglycerides and glucose circulate in the blood, reflecting an excess of nutrient intake over expenditure. The excess glucose and lipids are metabolized into triglyceride for storage. Figure 1.2 summarizes the most important pathways that occur inside an adipocyte. These include de novo lipogenesis where glucose is converted to fatty acids via acetyl-CoA; glycerol synthesis from both glucose and pyruvate, and fatty acid esterification to form triglyceride.

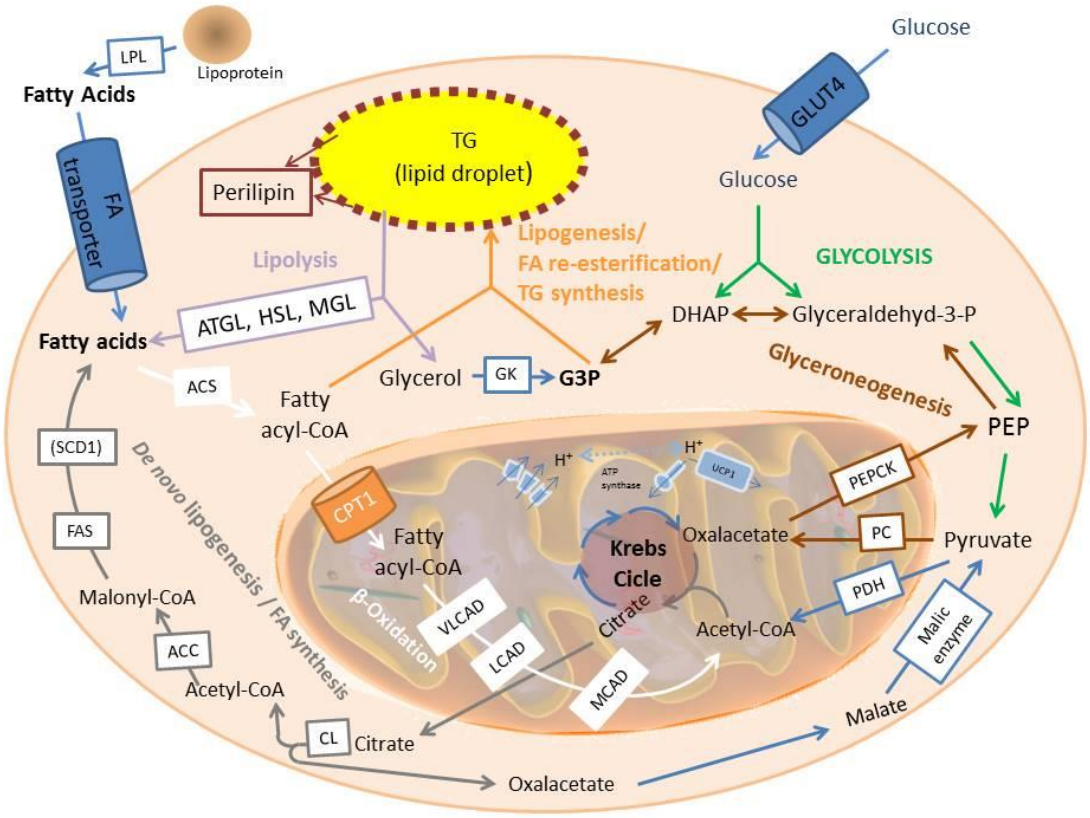

Figure 1.2 – Summary of the key metabolic pathways in an adipocyte [12, 13].

1.3.1 Fatty acid esterification

Fatty acid esterification represents a crucial metabolic pathway since it is by this process that triglycerides are synthesized. Triglycerides that are carried via lipoproteins circulating in blood are a principal source of FA for esterification. FA are liberated by lipoproteins in the presence of lipoprotein lipase (LPL) and they enter in the adipocyte via FA transporter proteins. After uptake, FA are converted to fatty acyl-CoA by acyl-CoA synthetase (ACS), and this reaction consumes 2 equivalents of ATP. The other element necessary to proceed with esterification is glycerol-3-phosphate (G3P). This precursor may have different origins, namely via glyceroneogenesis or glycolysis. Having the two main components, TGs are then created by series of reactions involving stepwise esterification of fatty acyl-CoA to G3P and dephosphorylation of glycerol. There are four enzymes that catalyse this fatty acid esterification process: glycerol-3-phosphate acyl transferase (GPAT), acylglycerolphosphate acyltransferase

(AGPAT), phosphatidate phosphatase and diacylglycerol acyltransferase (DGAT).

1.3.2 *De novo* Lipogenesis

FA used to synthesize TGs may also have an endogenous origin in a process called *de novo* lipogenesis. The precursor of FA synthesis is acetyl-CoA and it can be generated by catabolic process in mitochondria. However, it has to be transported to cytoplasm where FA synthesis takes place. Acetyl-CoA joins with oxaloacetate creating citrate that crosses the membrane via the tricarboxylic carrier and is cleaved to regenerate acetyl-CoA by ATP-citrate lyase (CL). Acetyl-CoA is converted to malonyl-CoA by acetyl-CoA carboxylase (ACC). A multimeric complex of fatty acid synthase (FAS) will process malonyl-CoA that will be incorporated in a growing chain of new FA. It was described in literature that the synthesis of a molecule of palmitate from acetyl-CoA requires 49 ATP [12]. It is possible to conclude that the *de novo* lipogenesis in adipose tissue represents a substantial energy-consuming pathway.

Palmitate, a 16-carbon saturated FA, is the primary product of FA synthesis. This compound can be elongated or dehydrogenated by the presence of different enzymes, the most common is Δ-9 desaturase-stearoyl-CoA desaturase (SCD1) [14].

G3P needs to be produced to allow TG synthesis. In the liver, this can be directly generated from glycerol via glycerol kinase (GK). However, GK is activity is low in other tissues including WAT. In WAT, G3P needs to come from dihydroxyacetone phosphate, and this compound may have two different origins, glycolysis and glyceroneogenesis.

1.3.3 Glycerol formation from glycolysis and glyceroneogenesis

Between these two pathways, glyceroneogenesis is the one that WAT uses more to obtain G3P [15]. The deuterium labelling patterns expected for

each of these pathways will also be further discussed. Glyceroneogenesis starts with pyruvate, whereby it is converted to oxaloacetate by pyruvate carboxylase (PC). Oxaloacetate is then converted to phosphoenolpyruvate (PEP), via phosphoenolpyruvate carboxykinase (PEPCK) - this step being considered to be rate limiting for the whole process.

1.3.4 Lipolysis

Lipolysis is another pathway present inside the adipocyte. In WAT, lipolysis allows the cell to produce free non-esterified FA (NEFA) used as an energy source for the tissues, particularly during fasting. While in BAT, lipolysis of stored TG is the predominant source of substrate for NST. The lipid droplet(s) contained inside the adipose tissue are covered by a layer of different proteins, the main component of which is perilipin. This layer dissociates from the surface of the droplet allowing lipolytic enzymes to access the triglyceride molecules. TG are hydrolysed stepwise, as shown in Figure 1.3. Initially the TG is converted into diacylglycerols in the presence of adipose triglyceride lipase (ATGL) and/or hormone-sensitive lipase (HSL). HSL is also responsible for catalysing the hydrolysis of diacylglycerols to monoacylglycerols. Lastly, the monoacylglycerols are converted by the calatizing presence of monoglyceride lipase (MGL).

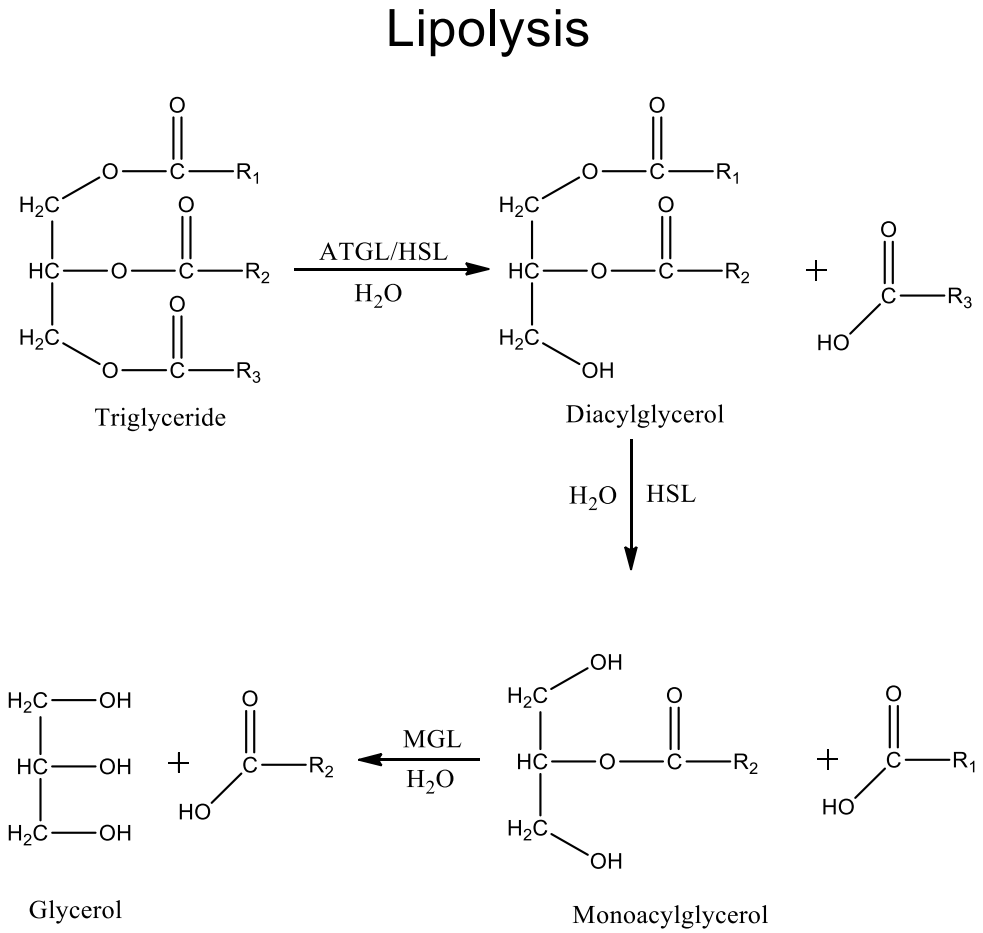

Figure 1.3 – Lipolysis overview mechanism.

1.3.5 β-Oxidation

The products obtained from the lipolysis of TG can be used for different purposes depending on the type of adipose tissue. The classical white adipose tissue releases most of the glycerol and FA into circulation. FA are transported to other tissues for energy generation, while glycerol is used by the liver as a substrate for gluconeogenesis. In BAT, fatty acids are consumed in mitochondria by a process called β-oxidation. After the activation of FA with ACS, the resulting fatty acyl-CoA is transported into the mitochondrial matrix via carnitine palmitoyltransferase 1 (CPT1). CPT1 is potently inhibited by malonyl-CoA, the product of acetyl-CoA carboxylation via acetyl-CoA carboxylase and the initial step of *de novo* lipogenesis. Thus, β-oxidation cannot occur if *de novo* lipogenesis is active. Inside the mitochondria fatty acyl-CoA undergoes a series of four reactions that shorten the FA chain by 2 carbons for each cycle creating

acetyl-CoA and the reducing equivalents NADH and $FADH_2$. The enzymes that catalyse β-oxidation belong to a family of acyl-CoA dehydrogenases (ACAD), that oxidize FA with various chain lengths: specifically very long chain ACAD (VLCAD), long chain ACAD (LCAD) and medium chain ACAD (MCAD).

In the majority of cells, the movement of electrons through the respiratory chain in inner mitochondrial membrane leads to the creation of ATP by a membrane enzymatic complex named ATP synthase. Whereas, in BAT the quantity of ATP synthase is small [16] and there is a high content of proton transporter UCP1. Mitochondrial uncoupling is a characteristic of BAT since the proton motive force is not coupled to ATP production but instead to heat production via proton flow through UCP1 [17]. As described, FA are the predominant subtract of thermogenesis in BAT. FA pool can produce electrons carriers for the respiratory chain but it also can serve as an activator of UCP1 [18].

During long term thermogenesis, the store of FA contained in the droplets of brown adipocytes is insufficient so the activity of LPL and FA/glucose uptake is rapidly increased after cold stimulus [19]. This uptake can increase to the extent that BAT can reduce significantly TG and glucose levels in plasma. This capacity has attracted the attention of researchers to understand BAT physiology and its possible role in counteracting obesity.

1.4 Triglyceride Futile Cycling

It is possible that there is another pathway used by adipocytes to dissipate ATP and therefore promote substrate oxidation. This pathway is a cycle where fatty acids and glycerol are generated from triglyceride lipolysis and are then re-esterified to triglycerides. ATP is consumed by both the synthesis of new glycerol-3-P and by the conversion of FA to FA-CoA. This pathway is called futile cycling of triglycerides and fatty acids.

The existence of this futile cycling is controversial and a key goal of our work is to develop novel methods to clarify its existence. Our approach is to measure the rate of the incorporation of newly-synthesized glycerol to the TG

pool using D_2O, on the basis that one turn of the futile cycle requires the synthesis of one glycerol-3-P molecule. Figure 1.4 provides a general description of how the experiment functions. Following TG lipolysis, three free fatty acids and one glycerol is generated. In the absence of glycerol kinase, glycerol cannot be phosphorylated hence glycerol-3-P has to be synthesized *de novo* in order for fatty acids to be converted back to the triglyceride. During *de novo* synthesis of glycerol-3-P, deuterium from body water is incorporated into hydrogens that are bound to the glycerol carbon skeleton. Thus the level of deuterium enrichment of the glyceryl moiety is proportional to futile cycling activity. Since futile cycling consumes energy, this needs to be balanced at some point by energy generation via substrate oxidation.

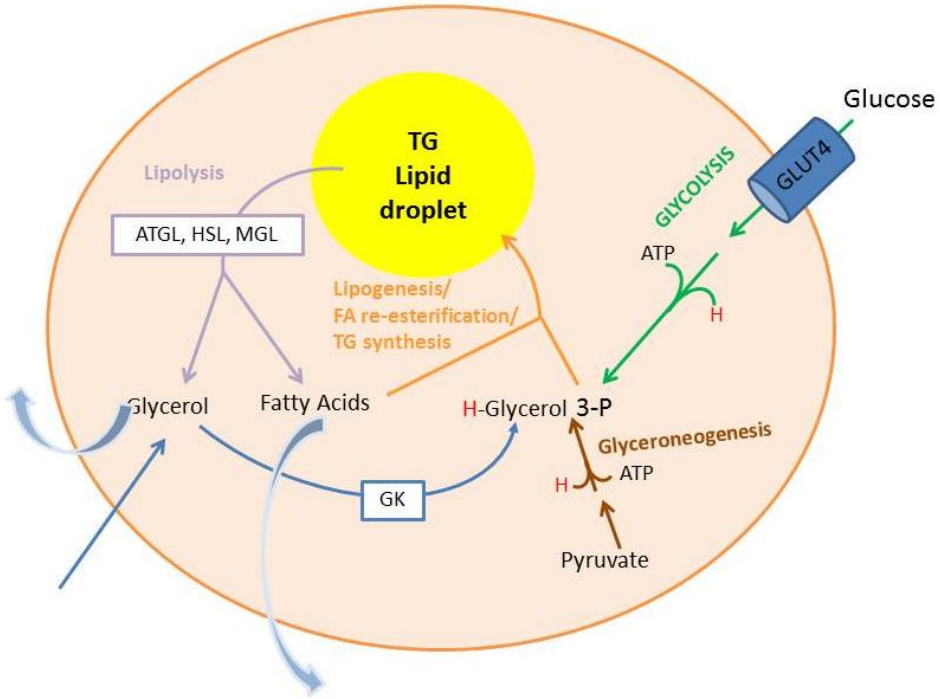

Figure 1.4 – Triglyceride labelling with deuterium during the futile cycling of triglycerides and fatty acids. The activity of GK can be neglected because in normal conditions it is very low.

.

1.5 NMR

NMR is a physical phenomenon based on the quantum mechanical magnetic properties of certain nuclei (spin quantum number ≠0) when placed in a strong static magnetic field (B_0). A proton behaves like a tiny bar magnet and has a magnetic moment associated with it. In the absence of an external magnetic field, the nuclear spins of the protons are randomly oriented. However, when an external magnetic field (B_0) is present, the nuclear spins are oriented so that the resulting nuclear magnetic moments are aligned either parallel or antiparallel to B_0 (z-axis). The orientation with lower energy associated is the one parallel to B_0, it is common knowledge that most nuclei have this orientation. Stimulation of the nuclei by an additional orthogonal oscillating radio frequency (RF) magnetic field (B_1) change the angle of alignment, transiently swings these nuclei out of alignment producing a magnetization vector (M) during a period of time (pulse), the bulk magnetization starts to process the transversal xy-plane. After this pulse, the bulk magnetization continues its original orientation along the z-axis linked with a time constant, T_1 relaxation time, with this is associated an emission of magnetic energy to the environment. The nuclei can also fall out of alignment with each other (spin-spin T_2 relaxation). The magnetic field associated with the new orientation of nuclear spins induces an electrical signal to the receiver that decreases with the time as the nuclei return to the original orientation. The result is a composite of decay patterns of all the protons in the molecule called free-induction decay (FID). This FID is recorder by the NMR spectrometer and when we apply the mathematical operation Fourier transform (FT) it will originate the corresponding spectrum. It is important to have in mind that each nucleus in a molecule resonates at a given but unique frequency and it depends on the molecular structure. This occurs because in different molecules, their nuclei experience slightly different magnetic field strengths depending on the shielding that nearby electrons confer. This characteristic of each nucleus is

called the chemical shift. NMR principles are summarized schematically in Figure 1.5.

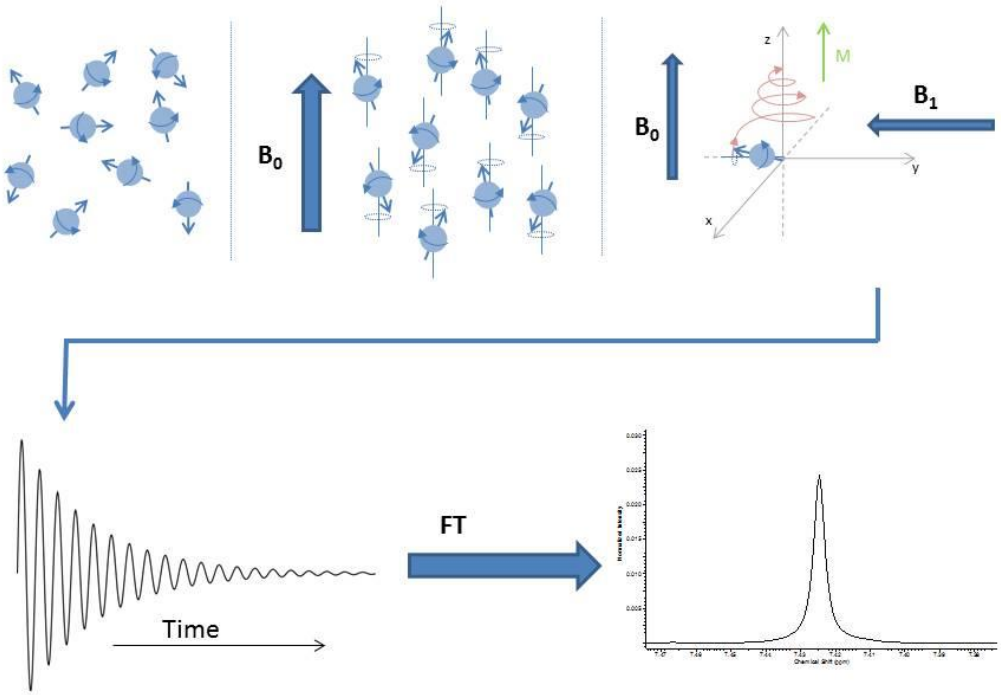

Figure 1.5 – Principles of NMR Spectroscopy.

Usually the NMR analysis can be done with nuclei that have a high natural abundance for example to identify the constituents of a certain sample. On the other hand, it is possible to use nuclei with a low natural abundance, called tracers, if the information requested is different such as the measure of the overall metabolic flux through the pathway given by the rate of conversion of the tracer from precursor to product, or even the contribution of a particular pathway to a product pool. There are many different tracers used to accomplish this objective. To be considered tracer, the nucleus in utilization has to have a spin different from 0, so it can be observed by NMR spectroscopy. Two of the most used isotopes are ^{13}C and ^{2}H because they are stable, non-radioactive and safe to be used in humans if it is needed. These isotopes can be monitored and detected using NMR spectroscopy for quantification of isotopic enrichment. NMR has a poor sensitivity but it can be overcome by the analysis of larger samples (10-100 μmol) and we can also analyse multiple stable isotopes or

labelling patterns used to probe different metabolic pathways. NMR is a non-destructive technique, hence the sample can be retained for repeated measurements.

1.5.1 ^{1}H-NMR

Hydrogen is the most sensitive nucleus for NMR analysis because it has a high gyromagnetic ratio and a high natural abundance (99.9%). This last characteristic combined with the fact that essentially all biological metabolites have bound hydrogens provides a rich source of information on the identification and quantification of a vast variety of metabolites by ^{1}H-NMR analysis.

1.5.2 ^{2}H-NMR

Deuterium has a spin quantum number (I) of 1 and consequently a magnetic quadrupolar moment. When compared to ^{1}H, the ^{2}H nucleus has shorter relaxation times that lead to broader NMR signals. Its gyromagnetic ratio is also only ~1/6th that of ^{1}H. Not only does this make it inherently less sensitive but its signal dispersion is only ~1/6th that of ^{1}H. Thus at 500 MHz, while the ^{1}H dispersion is 500 Hz/ppm, the corresponding ^{2}H dispersion is only 76.7 Hz/ppm. Consequently, effective separation of ^{2}H signals is dependent on spectrometers with fields of 11.7 Tesla or above (i.e. 500 MHz or higher for ^{1}H). The natural abundance of ^{2}H is 0.015%, providing a low background against which metabolite enrichment from $^{2}H_2O$ can be precisely quantified. When analysing NMR spectra, ^{2}H nuclei that are incorporated into metabolites have identical chemical shifts values as their ^{1}H counterparts since they share the same chemical environment. This characteristic allows the confirmation of the position of the ^{2}H in a molecule by intersecting the ^{2}H and ^{1}H NMR spectra.

The quadruploar nature of the ^{2}H nucleus makes it more susceptible to line broadening by restricted motion of the nucleus. The ^{2}H that are incorporated into the glyceride part of the TGs have much more restricted mobility compared to other sites, such as the FA methyl positions for example.

Thereby, for generating narrower and therefore better resolved signals, the glyceryl deuterium nuclei need to be in a smaller molecule that can more rapidly tumble in solution. Removal of the triglyceride fatty acid chains via transesterification achieves this objective.

The most straightforward way to incorporate ^{2}H into metabolites of living organisms is through the utilization of deuterated water ($^{2}H_2O$). Deuterated water was firstly used as a tracer in 1934 by George de Hevesy and Hoffer [20], to estimate the rate of turnover of water in the human body. Deuterated water is a safe and relatively inexpensive tracer that can be administrated orally or given as an intraperitoneal injection. The administered $^{2}H_2O$ rapidly equilibrates with total body water (BW) in all tissues. Following the initial loading dose, body water ^{2}H enrichment can be maintained indefinitely by drinking water enriched with a maintenance level of ^{2}H.In the presence of ^{2}H-enriched water, metabolite hydrogens that are bound to the carbon skeleton become enriched by reactions that involve hydrogen exchange or addition. At neutral pH, essentially all of these processes are mediated by specific enzymatic mechanisms rather than occurring spontaneously, hence the ^{2}H enrichment of metabolites from $^{2}H_2O$ indicates that they must have participated in or originated from one or more enzymatic reactions during the interval when $^{2}H_2O$ was present.

There is a published method that uses deuterated water and ^{2}H NMR spectroscopy with the purpose of obtaining the percentage of hepatic lipids that were *de novo* synthesized during the labelling period [21]. A basic description of this method is an initial injection of the mice with D_2O then these mice are returned to their cages and given unlimited access to deuterium enriched water to maintain the body water enrichment obtained by the initial injection, ~5%.

Quantification of TG futile cycling by this method allows us to test the effects of various interventions designed to alter its activity, most notably exposure to cold. Under these conditions mice need to increase lipolysis in white fat in order to supply energetic sources (free fatty acids) for brown fat thermogenesis. Futile cycling may also contribute to energy dissipation under these conditions.

In figure 4.3 on the bottom spectrum it is possible to see that the signals corresponding to hydrogens attached to carbons 1 and 3, of the glyceryl moiety, are very broad, makes quantification less accurate. The reason why these glycerol signals are intrinsically broad is because of the limited mobility of the nuclei since they are in the center of the large TG molecule. A previous study showed that ^{2}H-NMR spectroscopy of free glycerol yielded narrower signals compared with triglyceride-bound glycerol [22].Therefore, we reasoned that it would be easier to quantify the ^{2}H-enrichment level at the triglyceride glyceryl sites if the fatty acid chains were removed. As an illustration, the spectra shown in Figure 4.5 illustrate the difference between the ^{2}H NMR signals of triglyceride-bound glycerol and those of the same sample after the removal of fatty acids by transesterification.

1.5.3 Expected enrichment of glycerol from deuterated water

During futile cycling between triglyceride and fatty acids, the synthesis of triglyceride requires newly-synthesized G-3-P. Adipocytes can synthesize G-3-P from glucose via glycolysis and from pyruvate via glyceroneogenesis. Figures 1.6 and 1.7 show the two pathways and the theoretical exchanges that incorporate ^{2}H from water into specific hydrogens of G-3-P.

It is essential to note that the labelling patterns in both figures consider that none of the initial substrates are labelled. After a few hours, the organism reaches a steady-state where all the substrates will be in some way labelled. If this happens the labelling patterns will be altered and at a certain point it will be difficult to understand its origin.

Figure 1.6 shows the mechanism of glycolysis and it possible pattern of 2H-enrichment via glycolysis. This pathway starts with the phosphorylation of glucose through the action of enzyme hexokinase forming glucose-6-phosphate (G-6-P). This step is negatively regulated by the presence of glucose-6-phosphate. G-6-P is then converted into Fructose-6-phosphate (F-6-P) by phosphoglucoisomerase. A new phosphorylation happens at carbon 1 position

of F-6-P via the enzyme phosphofructokinase creating fructose-1,6-bisphosphate (FBP). This compound is then cleaved into two three carbon molecules: dihydroxyacetone phosphate (DHAP) and glyceraldehyde-3-phosphate (GA-3-P) by the presence of fructose bisphosphate aldolase. This step also results in the exchange of deuterated water and the enrichment of the position 4 glucose hydrogen. When FBP is cleaved, this enrichment is preserved in the hydrogen 1 of GA-3-P. GA-3-P is converted into DHAP by triose phosphate isomerase and at the same time, deuterium is incorporated into the other prochiral hydrogen 1 of DHAP. DHAP in then converted to glycerol-3-phosphate (G-3-P) by the presence of glycerol-3-phosphate dehydrogenase and NADH. Since the NADH hydrogen is rapidly exchanged with that of body water, it is enriched with deuterium and thus its transfer to hydrogen 2 of G-3-P results in enrichment of this position. Note that the pair of hydrogens at G-3-P position 3 is not enriched via glycolysis if the glucose precursor is unlabelled. However, with *in situ* administration of deuterated water, glucose hydrogens become extensively enriched with deuterium due to glucose turnover. Therefore under the experimental conditions, it is likely that the G-3-P position 3 hydrogens are also enriched.

The mechanism of glyceroneogenesis and it possible pattern of labelling is presented in Figure 1.7. On conversion of fumarate to malate by the enzyme fumarase, the deuterated water that enters in this step will label malate with one hydrogen. This reaction is reversible and it is a rapid equilibrium obtaining the molecule of malate labelled with two hydrogens at the same carbon. The oxidation of malate to oxaloacetate happens in the presence of malate dehydrogenase. Oxaloacetate is then decarboxylated by phosphoenolpyruvate carboxykinase and becomes 2-phosphoglycerate. This compound is converted to 3-phosphoglycerate via phophoglyceromutase. 3-phosphoglycerate is phosphorylated in carbon 1 by 3-phosphoglycerate kinase leading to 1,3-bisphosphoglycerate. This compound is then dephosphorylated in the presence of glyceraldehyde phosphate dehydrogenase to obtain glyceraldehyde-3-phosphate. The remaining steps are similar to the ones previously described and it will label the molecule at the carbon 2. Thus, glyceroneogenesis results in

the enrichment of all five hydrogens of G-3-P and glycerol from deuterated water.

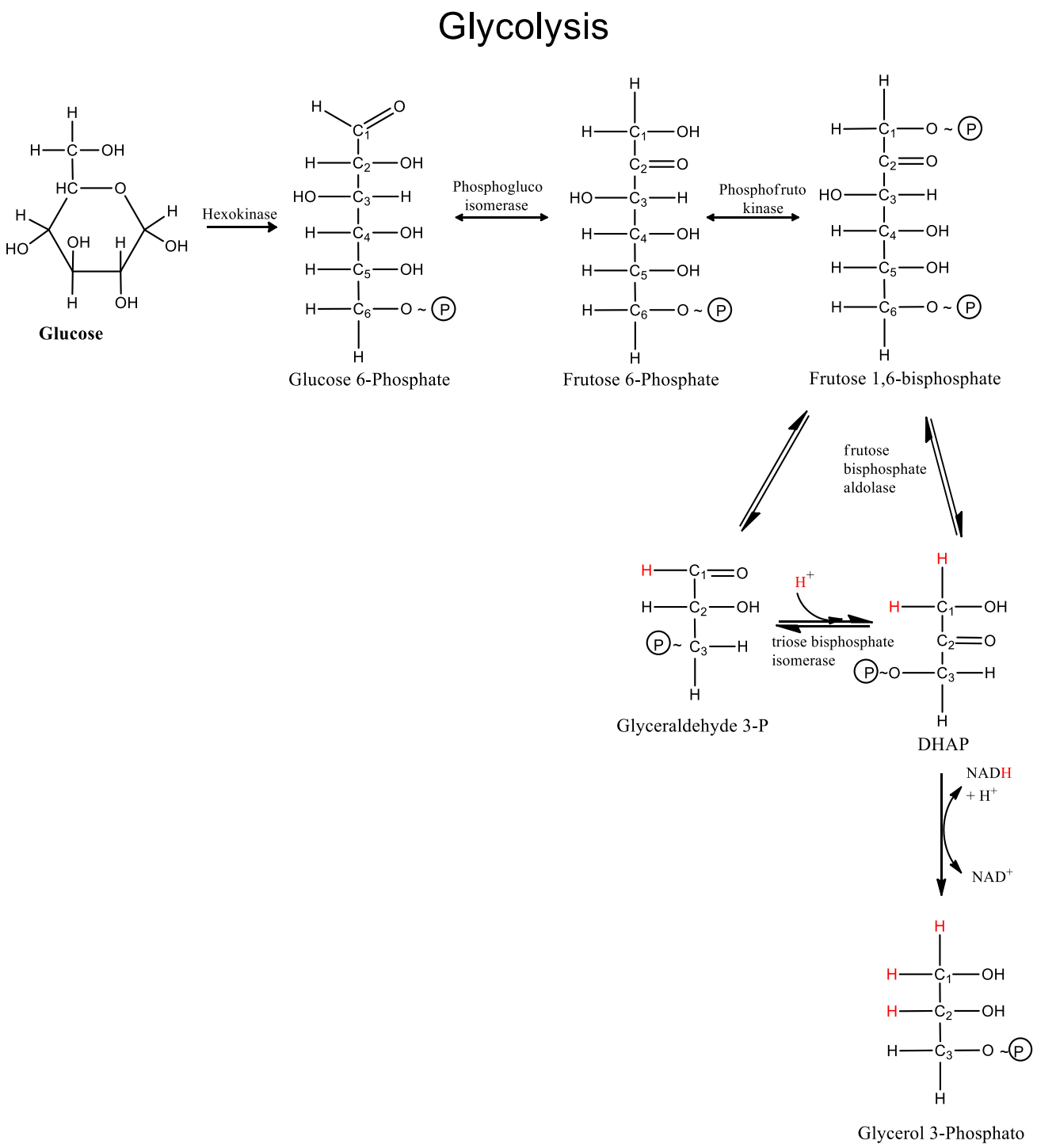

Figure 1.6– Summarized glycolysis mechanism and possible patterns of labelling. Adapted from [23].

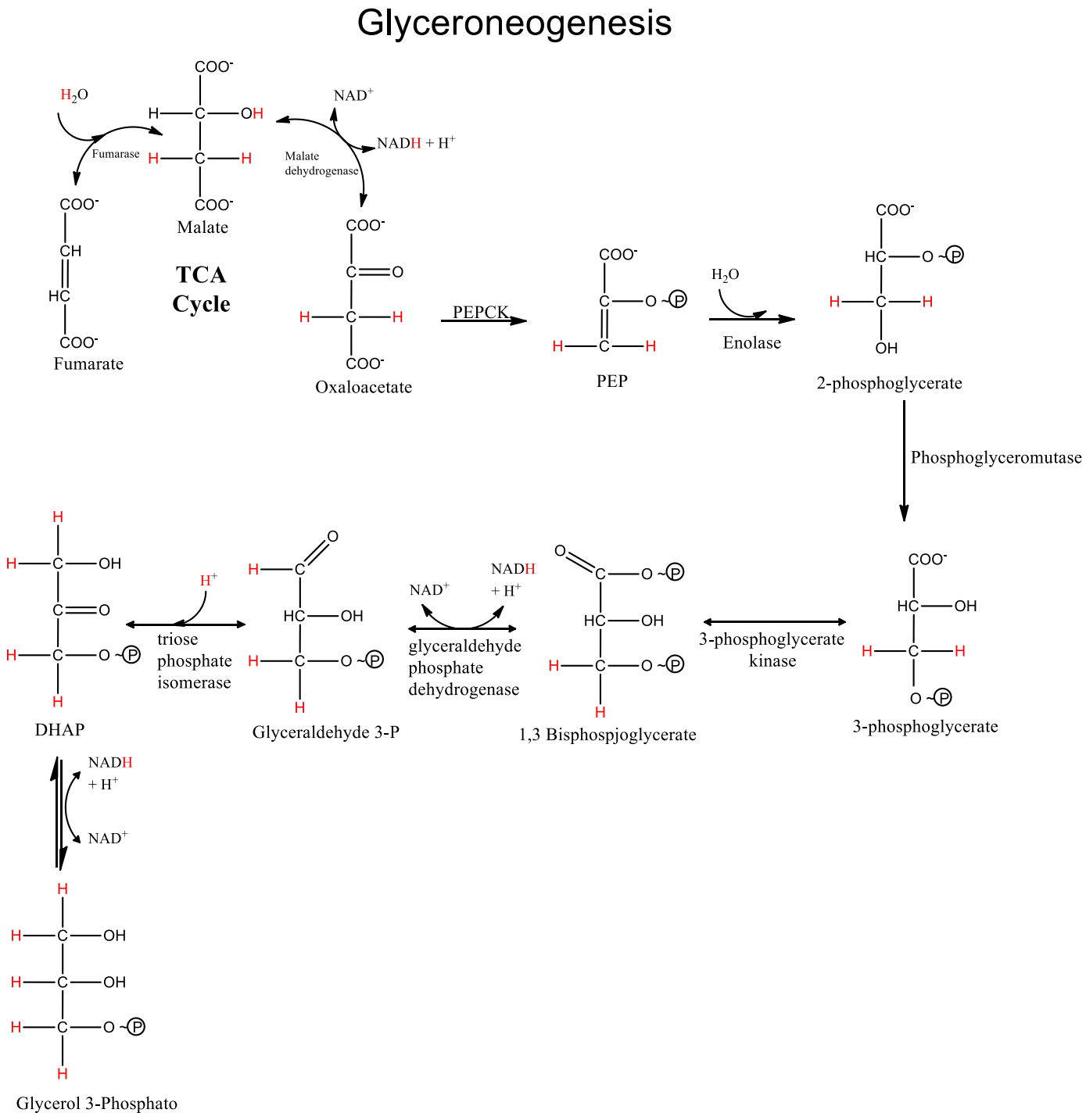

Figure 1.7 – Glyceroneogenesis pathway showing the steps where 2H is incorporated from $^{2}H_2O$ into the metabolic intermediates.Adapted from [23].

2. Aims of the dissertation

This project's aims are to test the hypothesis that triglyceride cycling in mice is a) promoted by cold conditions and b) shows differences between mouse strains that may be related to inherent differences in metabolic efficiency. To test this hypothesis, two strains of mice (C57BL/6 and AJ) were administered with D_2O under normothermic and hypothermic conditions and adipose tissue and plasma were harvested. Our role was to isolate the glycerol from the adipose tissue triglyceride and quantify its enrichment by ^{2}H NMR. Considering that we have limited amounts of hydrolysable triglyceride glycerol in the samples, we needed to optimize this process to obtain quantitative yields. We also have to take in account that the glycerol is analysed in aqueous solution hence the internal standard and fluorine lock had to be developed for this condition (previous samples have all been acquired in organic solvents). Thus, we pursued the following Specific Aims:

Aim 1: Optimize the protocol of TG transesterification to obtain maximal yields of purified glycerol.

Aim 2: Optimize ^{2}H NMR spectroscopy of the isolated glycerol to quantify ^{2}H-enrichment in the various hydrogens.

Aim 3: Quantify the fraction of adipose triglyceride glycerol that was newly synthesized during administration of $^{2}H_2O$ to mice that were kept under normothermic and hypothermic conditions. This fraction of synthesized glycerol is assumed to be equivalent to the fraction of triglyceride that underwent futile cycling.

Aim 4: Determine if normothermic and hypothermic futile cycling rates differ between C57BL/6 and AJ mouse strains.

3. Methods

3.1 Materials and equipment

The research done for this dissertation was performed in collaboration with Petr Zouhar Ph.D. and Pavel Flachs Ph.D. (Institute of Physiology of the Czech Academy of Sciences). Some parts of the design experiment were developed in Czech Republic by Petr Zouhar. These parts were: the animal exposure to cold, the tissue collection, and TG purification with Folch extraction and solid phase extraction [24].The materials and equipment used to perform these procedures will not be referred to in this Thesis.

Table 3.1 – List of materials used.

Material	Supplier
Acetic acid	Sigma
Acetone	Sigma-Aldrich
Benzene	Sigma-Aldrich
Chloroform	Panreac
Pyrazine-d4 98atm %D	Aldrich
Diethyl ether	Merck
Dowex 50x8-200	Sigma-Aldrich
Glyceryl tripalmitate	Sigma
Glycerol	Sigma
Glyceryl tristearate	Sigma
Hexafluoroacetone	Aldrich
Hexafluorobenzene	Sigma
Hexane	Sigma
Methanol	Panreac
Petroleum ether	Sigma-Aldrich
Pyrazine	Alfa Aesar
Sodium methoxide	Sigma-Aldrich
Tetrahydrofuran	Sigma-Aldrich
Water deuterium depleted	CortecNet

Table 3.2 – List of equipment used.

Equipment and Software	Supplier
ADC/Labs NMR Processor	Advanced Chemistry Development, Inc.
Varian VNMR 600 MHz	Varian
Bruker Avance III HD 500 MHz system	Bruker
Discovery DSC-Si SPE Tubes	Sigma
Genevac evaporator	Genevac
Heating plate with magnetic stirrer	Cole Palmer
Mini centrifuge	Labnet
Centrifuge	Sigma
pH meter	Jenway
Prism 6	GraphPad Software
Rotary evaporator	Büchi
Ultrasound bath	Branson
Vortex mixer	Falc

3.2 General description of experiments implemented

For the animal studies in Prague, the following protocol was performed: 6-week-old male mice of B6/J and AJ strain were co-caged in groups of three and kept in thermoneutral temperature (30 ºC) at least for 1 week. After that, some animals were maintained as controls in thermoneutrality (9 mice of each strain), whereas others were transferred to 4 ºC and left in this condition for two or seven days (9 or 6 mice of each strain, respectively; see Figure 3.1). Mice were fed by standard chow diet (STD) diet during the whole experiment.

In the first set of experiments, mice were injected with saline in deuterium oxide (9 $mg.l^{-1}$ NaCl, 99.9% $^{2}H_2O$), 40 hrs prior to dissection, in order to reach 3-5% ^{2}H-enrichment of body water. Following this loading dose, mice were then allowed unlimited access to 5% deuterium enriched drinking water to maintain their body water enrichment. In the second set of experiments, only two groups (thermoneutrality and 7 days of cold exposure) were used and $^{2}H_2O$ was injected 4 days before dissection (see Figure 3.1, the bottom part). After 7 days, mice were dissected in random fed state and blood and fat depots were

collected. Samples of eWAT and plasma aliquots were sent to Portugal and TG was purified from eWAT and analysed by ^{2}H-NMR.

AJ mice represent an obesity-resistant phenotype while B6 mice are

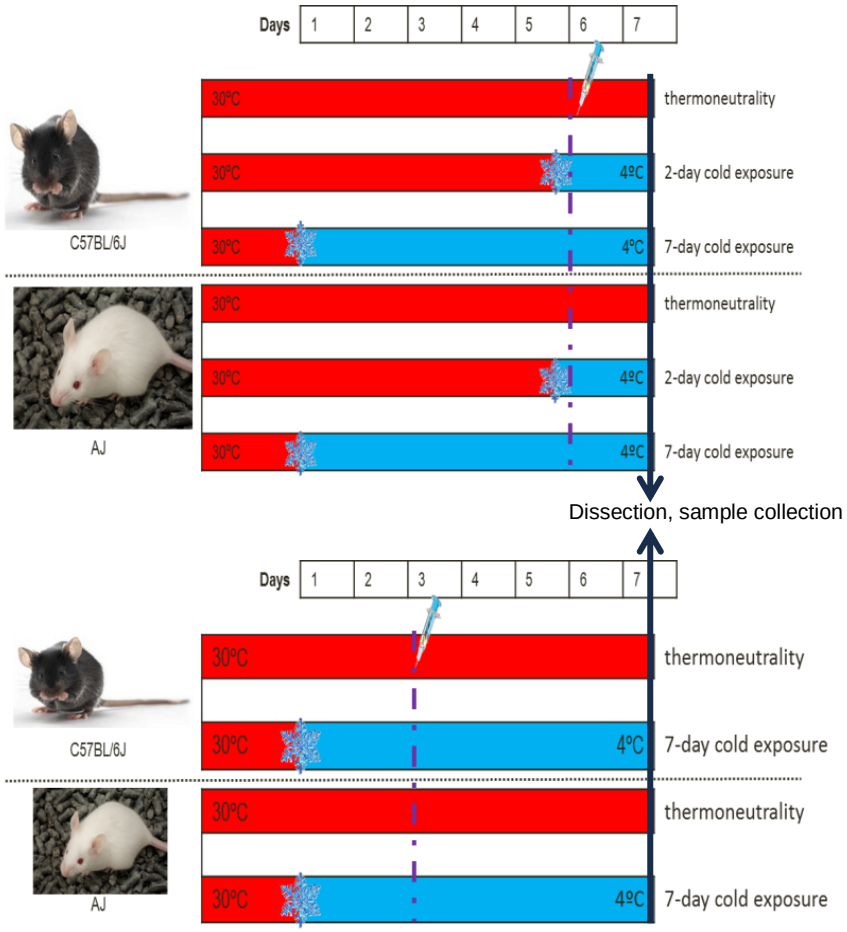

more prone to obesity development. Both strains are widely used in metabolic studies.

Figure 3.1 –Chronogram of experiments [12].

3.2.1 Optimization of triglyceride transesterification

For transesterification, we chose a previously described protocol for TG hydrolysis using sodium methoxide in methanol [25]. A commercial TG sample used to initially test the yields and optimize the conditions of the procedure. During this optimization, process different parameters (TG concentration, TG

solubilization, time of esterification, temperature etc.) were systematically changed with the purpose of obtaining the best yield possible.

The final optimized protocol was as follows: The triglyceride fraction was partially dissolved in 3 ml of methanol and trans-esterified by incubation with 2 ml of 0.5 N methanolic sodium methoxide at 55°C for 2 hours with magnetic agitation. After cooling to room temperature, the solution was mixed with 4 ml of water and 5 ml hexane. The mixture was centrifuged at 7700 rpm for 40 min. The two layers were separated with the hexane fraction containing the fatty acid methyl esters (FAME). The aqueous fraction containing the glycerol was passed through 1.5 ml Dowex-50-H+ resin and the pH adjusted to 7.0 with 0.01M sodium carbonate. The neutralized solution was evaporated in Genevac at 35ºC.

The mechanism that represents the reaction of transesterification is presented in figure 3.2. One of the carbonyl carbons will suffer a nucleophilic attach by the methoxide to form tetrahedral intermediate. This reaction can be reverted or it continues and the fatty acid methyl ester will be eliminated. The compound remaining compound is protonated originating a diglyceride. This will pass through the same steps until we obtain glycerol and two more fatty acid methyl esters.

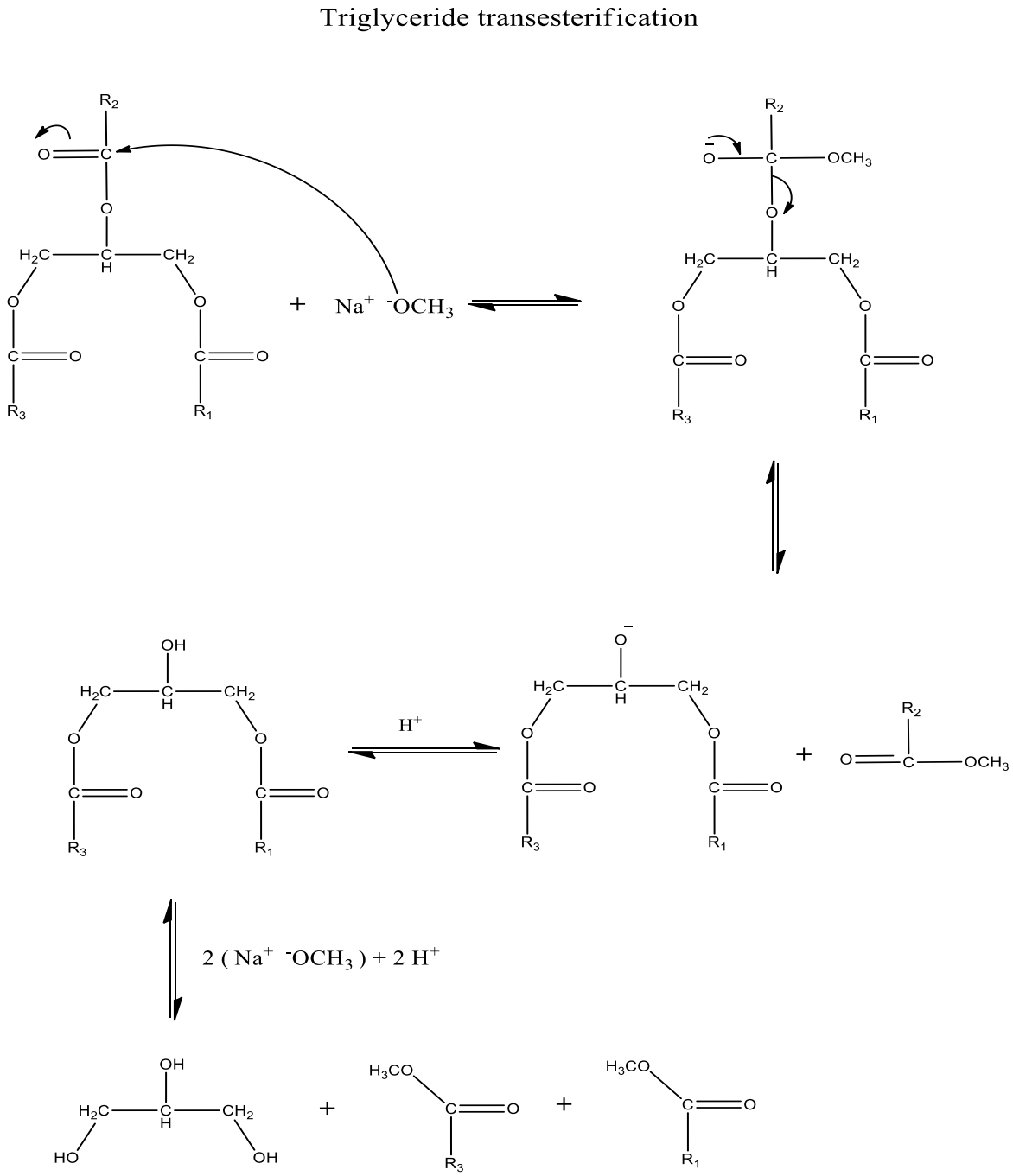

Figure 3.2 – Triglyceride transesterification mechanism.

3.2.2 ^{2}H NMR analysis in aqueous medium

Previous to this work, all ^{2}H NMR spectroscopy by the Lab had been performed in organic solvents. The preparation of a pyrazine standard that could be used in samples that are in aqueous phase was one of the priorities since the compound in study, glycerol, is soluble in water. The utilization of a fluorine containing compound soluble in water to offer the ^{19}F field-frequency lock to the NMR was also critical. The pyrazine standard was prepared with the following components: 2.68566 g pyrazine; 0,000419 g d_4-pyrazine, 98%-enriched, and 25 g of deuterium-depleted water. For ^{19}F lock, we added 50 µl hexafluoroacetone to each sample.

3.2.3 Deuterium NMR analysis

The samples were analysed by ^{1}H and ^{2}H-NMR spectroscopy using a Bruker Avance III HD 500 MHz system equipped with a 5-mm ^{2}H-selective probe with ^{19}F lock and ^{1}H-decoupling coil.

For ^{1}H acquisition, a spectral width of 10 kHz was used in conjunction with the acquisition pulse parameters. For ^{2}H acquisition, a spectral width of 921 Hz was used and broadband ^{1}H-decoupling was continuously applied. For maximizing signal-to-noise ratios of the glyceryl moiety, spectra were acquired under partial saturation conditions. Six of the samples were also acquired under fully relaxed conditions in order to obtain a correction factor for saturation. The acquisition pulse parameters are described in table 3.3. The samples were run at a temperature of 25ºC.

Table 3.3 – Parameters utilized in NMR acquisitions.

Spectrum	Number of scans	Pulse	Acquisition time [2]	Pulse delay [2]	Standard	Evaluated chemical group	Chemical shift (ppm)
^{2}H plasma spectrum	16	3µs 30º	4	8	Acetone	H_2O	
^{1}H TG spectrum	4	14.8 µs 90º	3	5	Pyrazine in chloroform	C1+C3 glycerol	4.1-4.4
^{2}H TG spectrum	5500	12 µs 90º	0.5(partially saturated) 1 (fully relaxed)	0.1(partially saturated) 8 (fully relaxed)	Pyrazine in chloroform	C2 Glycerol	5.37
						C1+C3 Glycerol	4.25
						FA methyl	0.84
^{1}H Glycerol spectrum	4	5 µs 30º	3	5	Pyrazine in water	C1+C3 glycerol	3.4-3.6
^{2}H Glycerol spectrum	5120	12 µs 90º	0.5	0,1	Pyrazine in water	C2 Glycerol	3.68
						C1+C3 Glycerol	3.4-3.6

Spectra were analysed using the curve-fitting routine supplied with the ACD/Labs 1D NMR processor software. [^{1}H] and [^{2}H] molar amounts were calculated from peak area with respect to the peak of the pyrazine $^{1}H/^{2}H$ standard.

3.2.3.1 Sample preparation for ^{2}H-NMR

To prepare each sample to NMR we applied the following protocol: 25 µL of pyrazine enriched with $^{2}H_4$-pyrazine standard dissolved in deuterium depleted water, 50µL of hexafluoroacetone, and 300 µL of water were added to the dried sample. Isolated TG were dissolved in 600 µl chloroform and mixed with 50 µl hexafluorobenzene and 25 µl pyrazine enriched with $^{2}H_4$-pyrazine standard also dissolved in the same chloroform.

Samples of plasma were prepared using the following steps: 10 µl plasma, 50 µl hexafluorobenzene, and 1 ml acetone. With this analysis we determined $^{2}H_2O$ enrichment of body water as described previously [26].

3.3 Calculations

^{2}H Body water enrichment

$$Body\ water\ enrichment = \frac{[\ ^{2}H_2O]}{[\ ^{2}H_2O] + [\ ^{1}H_2O]}$$

Analysis of triglyceride Spectrum

Proton Spectrum

The proton spectrum allowed us to quantify the amount of unlabelled hydrogens bound to carbons 1 and 3 of the glyceride moiety of TG. The concentration of hydrogens from these positions was calculated using the mentioned area in comparison with the amount of standard added. Quantifications were adjusted for the number of hydrogens per mol of pyrazine standard (4) versus the number of hydrogens in the various sites of glycerol (four for C1+C3; one for C2).

Deuterium Spectrum

With the deuterium spectrum we got more direct information as the deuterium labelling in carbons 1 and 3 of the glyceride moiety, and the deuterium labelling in carbon 2.

These data, we were able to calculate excess enrichments and fractional turnover rates for the whole glyceride moiety, and both C1+3 and C2 of glycerol moiety (some of these results are presented in the appendix). To do so we used the following formulas:

$$Excess\ enrichment\ (\%)\ = \frac{[\ ^{2}H]}{([\ ^{2}H] + [\ ^{1}H])} \times 100 - 0.015$$

0.015 is the background level of deuterium enrichment

$$Fractional\ turnover\ rate\ (\%)\ = \frac{excess\ enrichment}{body\ water\ enrichment} \times 100$$

Analysis of free glycerol

The calculations involved are similar to the triglyceride glyceryl. The excess enrichments and fractional synthetic rates for both C1 + C3 and C2 of glycerol moiety were also calculated using the formulas mentioned. After having these results we compared the quantity of TG obtained from the direct analysis of TG and the analysis after transesterification of TG.

Figures 4.2 and 4.3 are representative ^{1}H and ^{2}H spectra with description of main peaks to TG analysis and Glycerol analysis, respectively. In figure 4.2 we can see the molecular structure of glycerol and in red and blue are represented the possible sites where deuterium can be incorporated. Theoretically, all hydrogens linked to the carbons would be labelled and that we give us a ratio of C2 over (C1+C3) of 0.25.

$$\frac{C2}{C1 + C3} = \frac{1}{4} = 0.25$$

3.4 Statistical treatment

Data were analysed by unpaired t-test or two-way ANOVA with Sidak's multiple comparisons test using Prism 6. The first test was used in the graphs from figure 4.7 and in the last graph from appendix we did two unpaired t-tests. While in the rest of the graphs were analysed by two-way ANOVA with Sidak's multiple comparisons test. The difference was considered statistically significant when $p<0.001$.

4. Results and Discussion

4.1 Optimization of TG transesterification

To know the yield of the initial protocol of TG transesterification we applied it to a known amount of commercial TG. The initial yields obtained were low (< 20%). When we were adding sodium methoxide to the TG sample we noticed that TG dissolution was incomplete. We attempted to improve TG dissolution by dissolving beforehand in compatible organic solvents before adding the methanolic sodium methoxide reaction solvent. When this was performed, the yields were substantially improved: 44% with THF, 83% with diethyl ether and 98% with methanol. We applied this optimized protocol to the isolated TG samples derived from the mice.

Figure 4.1 shows the yields obtained of the TG transesterification, i.e. the moles of glycerol recovered from the moles of triglyceride starting material. The process was found to be highly consistent and reproducible and gave an average yield of 80%. Moreover, the glycerol ^{1}H and ^{2}H NMR signals were well resolved and there was no significant interference from other resonances (Figure 4.2).

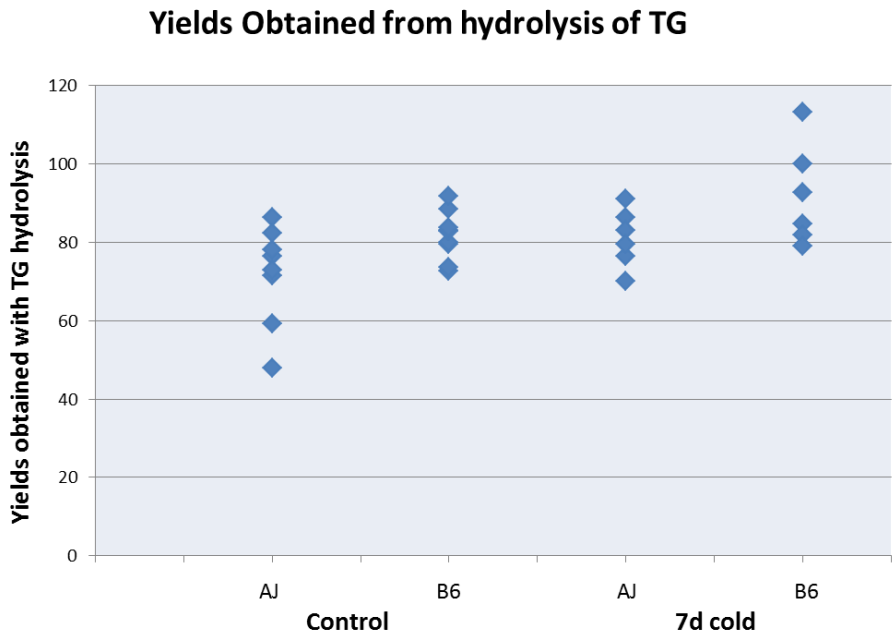

Figure 4.1 – Yield of TG transesterification.

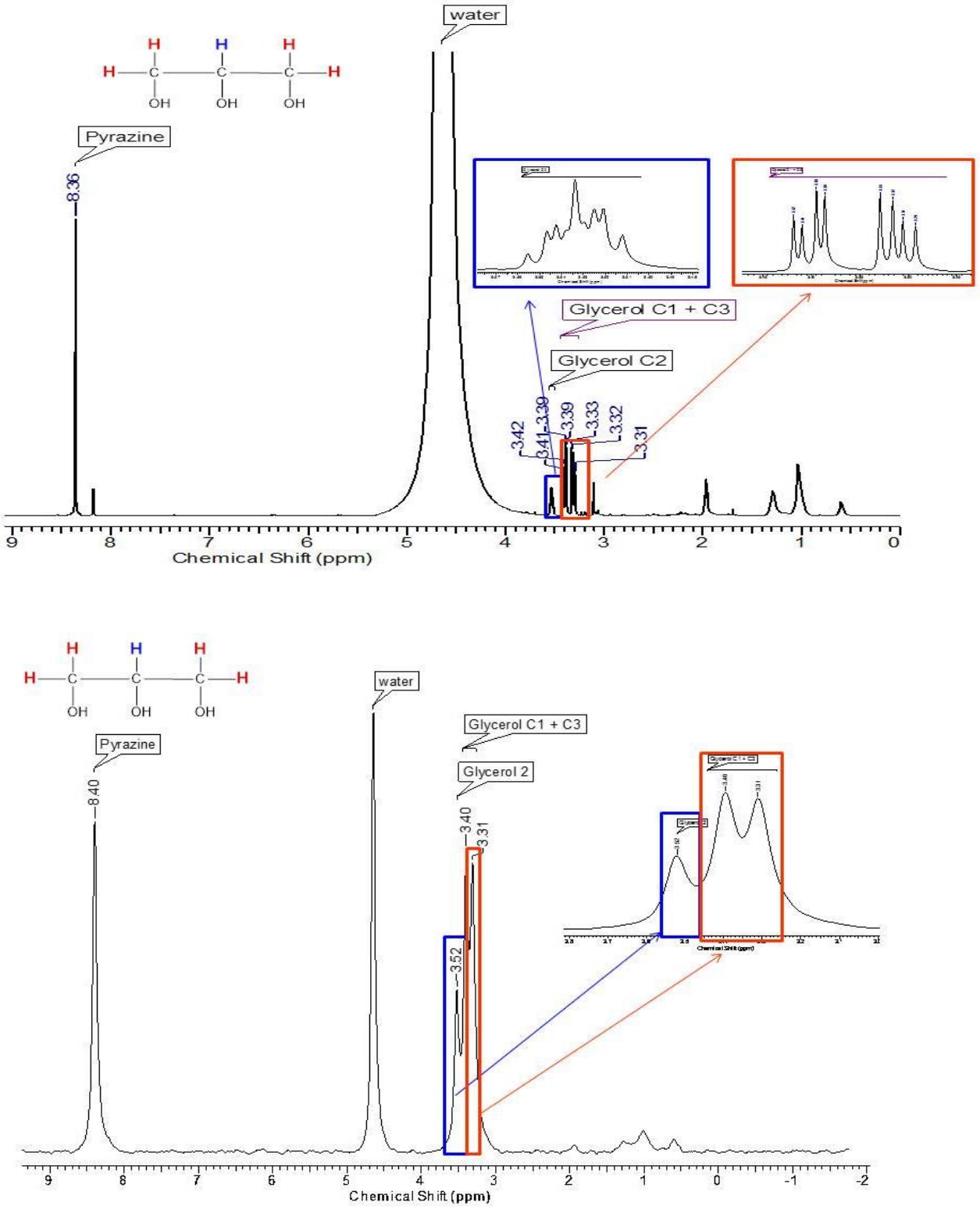

Figure 4.2 –Representative NMR spectra of glycerol obtained from TG transesterification. The top spectrum is from proton NMR and the bottom spectrum from deuterium NMR. Different colours represent hydrogens with different positions inside the molecule.

4.2 Analysis of the triglyceride spectrum

To verify that the ^{2}H-enrichment information of the TG glyceryl moiety was preserved following transesterification to glycerol, we obtained and analysed spectra from both the TG precursor and glycerol product. The TG precursor ^{1}H and ^{2}H NMR spectra are shown in Figure 4.3. While the well resolved glyceryl C1 + C3 signals at 4.1 ppm are well resolved in both ^{1}H and ^{2}H spectra, the linewidths of the glyceryl ^{2}H signals are noticeable broader compared to other signals, for example the fatty acyl CH_3. In addition to being broad, the glyceryl C2 resonance also overlaps with signals of olefinic hydrogens hence its enrichment cannot be reliably quantified. From the analysis of glyceryl ^{1}H and ^{2}H NMR signals, we determined the fractional synthetic rates of TG-Gly for the various conditions that the two strains of mice were subjected to, shown in Figure 4.4. The difference in fractional turnover rate between the control group and the group that were exposed to 2 days of cold temperatures was insignificant, while 7 days of cold exposure showed a substantial and significant induction of glyceryl turnover indicative of active TG-fatty acid futile cycling. While the two mouse strains had similar turnover rates under normothermic conditions, after 7 days cold exposure the AJ mice had significantly higher fractional turnover compared to C57BL/6 mice. To compare TG and isolated glycerol analyses, we focused on the samples representing control and 7 days of cold exposure. This way we were able to evaluate the analysis of isolated TG glycerol from samples covering the widest range of ^{2}H-enrichments.

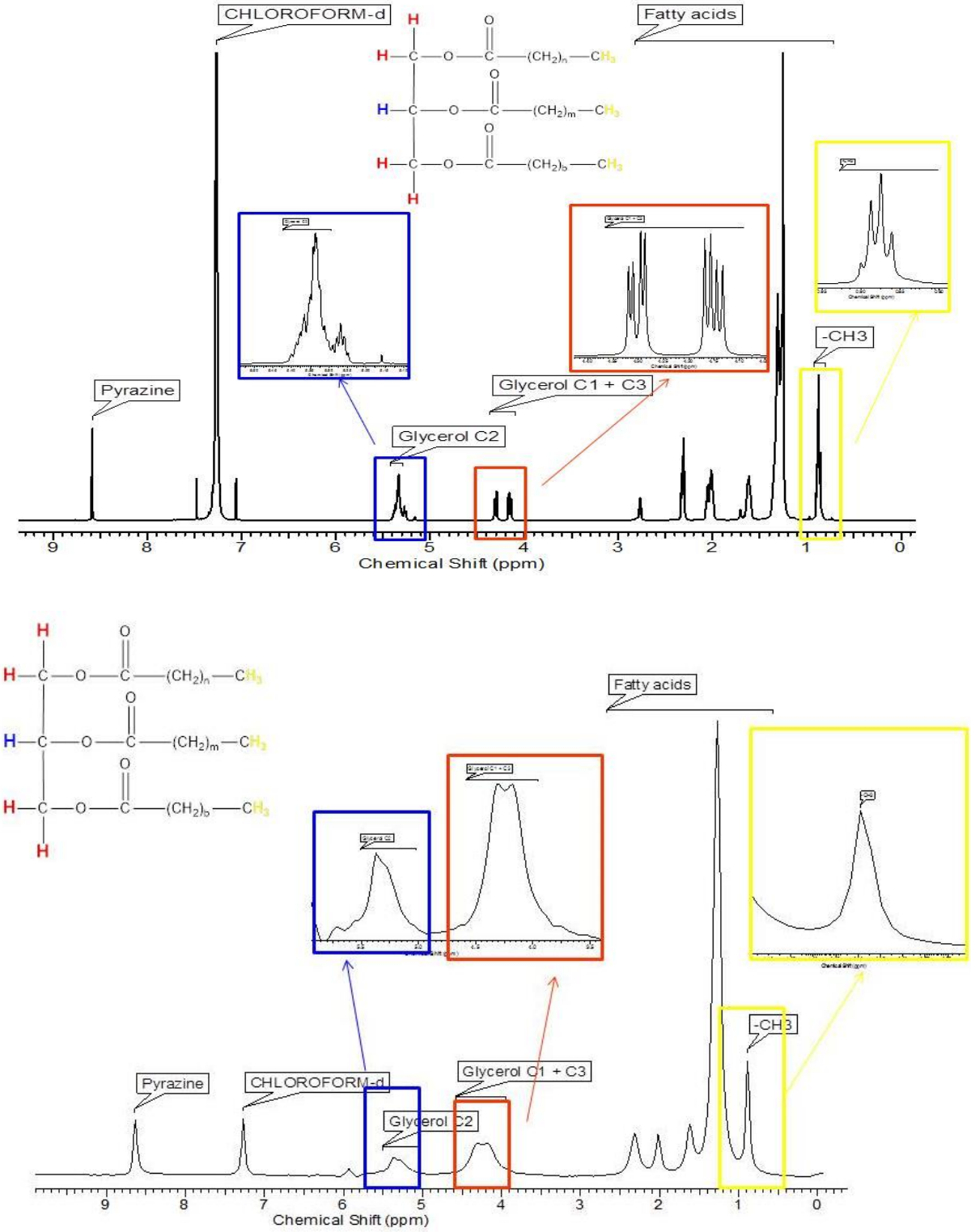

Figure 4.3 –Representative ^{1}H and ^{2}H NMR spectra of triglycerides. (Top and bottom spectra, respectively.) Different colours represent hydrogens with different positions inside the molecule.

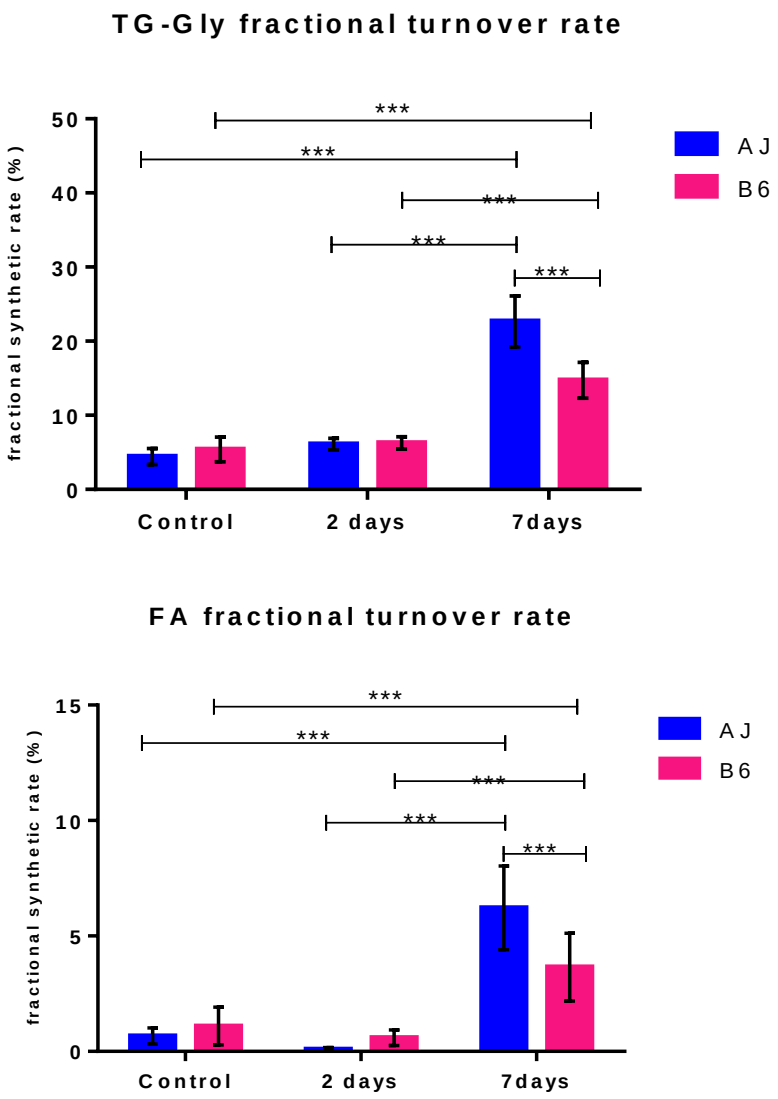

Figure 4.4–Fractional turnover rates of Glycerol and Fatty acids. Values are means corresponding to 9 mice (control and 2 days groups) and 6 mice (7 days group), with standard deviations represented by vertical bars.

**** Mean values were significantly different between the identified groups (P<0.001).*

4.3 ^{1}H/^{2}H NMR Analysis of isolated glycerol

Once the transesterification process was completed, ^{1}H and ^{2}H-NMR spectra were acquired technique using a Bruker Avance III HD 500 MHz system, mentioned in *chapter 3.2.3*.

When the NMR spectra of TG precursor and glycerol product are compared, (Figure 4.5) the improvement in resolution and signal-to-noise of the ^{2}H signals of free versus bound glycerol is noticeable. With free glycerol, it was possible to resolve three signals: the upfield signal corresponding to the hydrogen bound to carbon 2 of glycerol; and a pair of downfield signals corresponding to the prochiral *R* and *S* hydrogens bound to carbons 1 and 3. The chemical shifts and assignments are shown in the following table:

Table 4.1 – Chemical shifts and ^{2}H-linewidths of triglyceride-glyceryl and free glycerol resonances observed in 500MHz ^{1}H and ^{2}H-NMR spectra.

Nucleus	Compound	Solvent	δ (ppm)	Assignment	^{2}H-Linewidth (Hz)
^{1}H	TG-glyceryl	Chloroform	4.15	H3S, H1R	
			4.39	H1S, H3R	
	Free glycero	Water	3.46	H3S, H1R	
			3.55	H1S, H3R	
^{2}H	TG-glyceryl	Chloroform	4.25	H1S, H3R, H3S, H1R	14,23
			5.37	H2	19,46
	Free glycero	Water	3.47	H1S, H3R,	3,85
			3.55	H3S, H1R	3.68
			3.68	H2	3.41

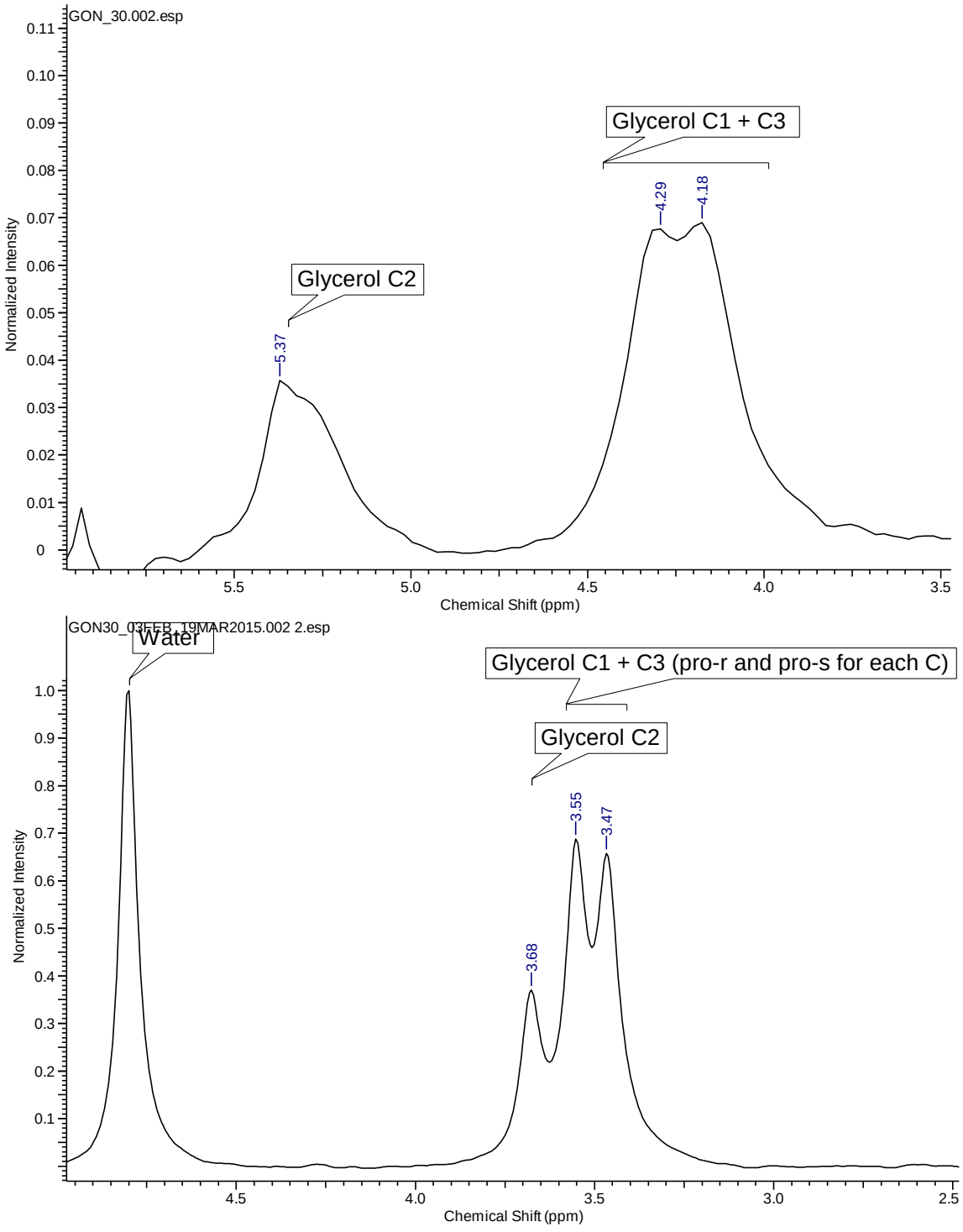

Figure 4.5 – 2H-NMR spectra from the exact same sample before (top) and after TG transesterification (Bottom).

The results obtained from the transesterification of TG are shown in figure 4.6. The estimates are consistent with those obtained from the intact TG demonstrating that the transesterification protocol preserved the ^{2}H-enrichment information of the TG glyceryl moiety.

The statistical tests performed do not show differences between TG and glycerol analysis, the p values are the same (0,0001) for the same set of samples. The coefficient of variation for the TG analysis after 7 days of cold exposure are 15,12 and 16,43% for AJ and B6 strain, respectively. For the glycerol analysis the values obtained were 15,83 and 22,87% for the same conditions and strains, in the same order. This outcome does not emphasize any considerable difference about the precision of the transesterification process.

The glycerol analysis also allows a more precise assessment of C2 enrichment since in the TG molecule, this signal overlaps with those of olefinic hydrogens, which can themselves be enriched from $^{2}H_2O$.

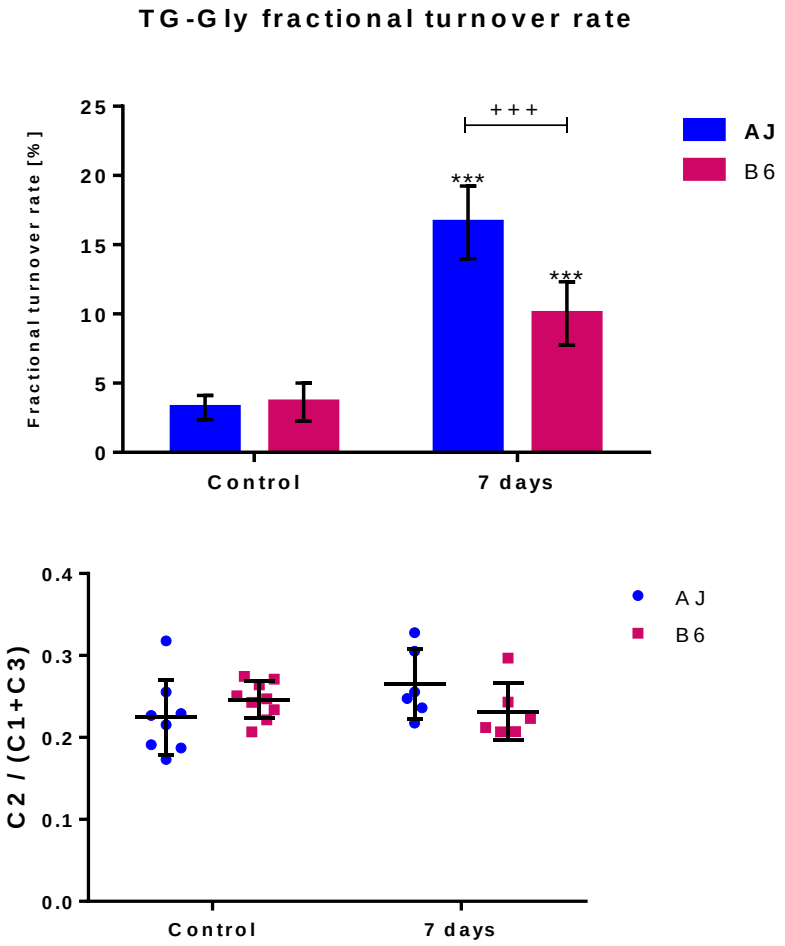

*Figure 4.6 - Fractional synthetic rate of glycerol and C2 over C1 plus C3 ratio. Values are means corresponding to 8 mice for the AJ and 9 mice for the B6 (control groups) and 6 mice (7days group), with standard deviations represented by vertical bars.*** Mean values were significantly different from those of control animals (P<0.001).+++ Mean values were significantly different between the animals of 7 days groups. (P < 0,001).*

An additional set of samples obtained from AJ mice were also analysed by NMR before and after TG transesterification (control and 7 days groups). The mean transesterification yields were comparable to those of the previous study (86%) indicating the good reproducibility of this protocol. Figure 4.7 shows the fractional synthetic rate of glycerol and the ratio of C2/(C1 +C3) enrichments. These results are concordant to the previous ones by having a synthetic rate of glycerol higher after 7 days of cold exposure.

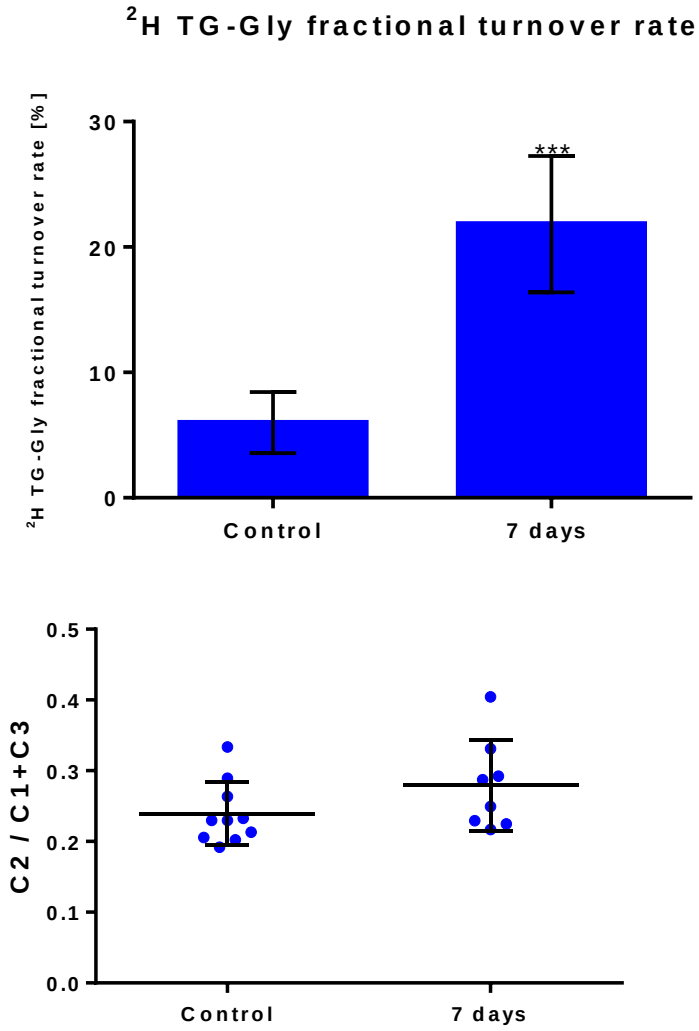

*Figure 4.7 -- Fractional synthetic rate of glycerol and C2 over C1 plus C3 ratio. Values are means corresponding to 9 mice for control groups and 8 mice for 7 days group of AJ strain, with standard deviations represented by vertical bars.*** Mean values were significantly different from those of control animals (P<0.001).*

In figures 4.6 and 4.7 are represented the ratio of C2 over the sum of C1 and C3. It is possible to note that the mean of this ratio is around 0.25 in both set of samples. The statistic test utilized in each one of them showed that there is no statistical difference between the groups.

Theoretically, if all the glycerol sites are equivalently enriched from $^{2}H_2O$, then the ratio of C2 to (C1 + C3) enrichments should be 1:4, or 0.25. As shown in Figure 4.6, the distribution of glycerol enrichment did conform to this pattern,

indicating that newly synthesized glycerol was not preferentially enriched in one hydrogen site over another. According to the labelling patterns presented in figures 1.6 and 1.7 the most likely origin for glycerol labelled in all 5 hydrogens is glyceroneogenesis. However, glycerol generated from glycolysis of glucose that was already enriched with deuterium would also have all hydrogens enriched. Previous studies using Mass Spectrometry present results similar to the ones obtain with this study [23]. The bottom graph of figure 4.6 shows that in some samples the ratio can be higher than 0,3 which means that the have the hydrogens of C3 + C1 less labelled compared with C2; and in other cases we have values lower than 0,2 meaning the exact opposite. If the only pathway contributing to the TG labelling was the glyceroneogenesis, all the hydrogens would be labelled. Aside from the uncertainty of NMR signal measurements, the differences observed may also be explained by the contribution of other pathways such as glycolysis, this would reduce the labelling in carbon 3; or the direct conversion of glycerol present inside the cell in G-3-P via glycerol kinase. Although glycerol kinase activities are thought to be low in adipose tissue, recent evidence suggests that this enzyme might be upregulated in BAT and perhaps even in Brite tissues. To the extent that glycerol kinase participates in futile cycling, enrichment of triglyceride glyceryl C1+C3 from deuterated water will underestimate the true rate of cycling since glycerol conversion to G-3-P via glycerol kinase does not result in enrichment of any of these hydrogens with deuterium. However, since G-3-P is known to be in rapid equilibrium with DHAP, this would result in the enrichment of carbon 2, but no other sites. These mechanisms could explain how experimental glycerol C2/(C1+C3) enrichment ratios vary from the theoretical value of 0.25.

Conclusions and future perspectives

In conclusion, we were able to improve the analysis of triglyceride glyceryl enrichment by ^{2}H NMR by the analysis of free glycerol following triglyceride transesterification. This analysis also required the development of a new ^{2}H NMR protocol for the study of aqueous samples, which will benefit other projects in the future. With this methodology, we were able to demonstrate and quantify TG/NEFA futile cycling in mice.

One interesting thing to do in the future would be adapt the protocol to use gas chromatography–mass spectrometry (GC-MS). This is a technique that has been reported and has having some benefits when compared with NMR. First of all, it is more sensitive being able to analyse smaller samples such as triglycerides obtained via biopsy sampling methods. Secondly, it consumes a smaller amount of time allowing higher throughput of samples. But it has disadvantages as well, in contrast to NMR it does not provide positional enrichment information and is destructive to the samples. If we were able to develop this technique we could follow the metabolism of animals in study during a longer period of time using via fine needle biopsy of the EWAT to analyse the metabolism. In this way we would avoid having to sacrifice the animal in order to obtain triglyceride.

List of figures

List of tables

References

1. Rajala MW and Scherer PE (2003) Minireview: The Adipocyte—At the Crossroads of Energy Homeostasis, Inflammation, and Atherosclerosis. Endocrinology 144:3765-3773. doi: doi:10.1210/en.2003-0580
2. Han TS, Lee DM, Lean ME, Finn JD, O'Neill TW, Bartfai G, Forti G, Giwercman A, Kula K, Pendleton N, Punab M, Rutter MK, Vanderschueren D, Huhtaniemi IT, Wu FC and Casanueva FF (2015) Associations of obesity with socioeconomic and lifestyle factors in middle-aged and elderly men: European Male Aging Study (EMAS). Eur J Endocrinol 172:59-67. doi: 10.1530/eje-14-0739
3. Himms-Hagen J, Melnyk A, Zingaretti MC, Ceresi E, Barbatelli G and Cinti S (2000) Multilocular fat cells in WAT of CL-316243-treated rats derive directly from white adipocytes.
4. Waldén TB, Hansen IR, Timmons JA, Cannon B and Nedergaard J (2012) Recruited vs. nonrecruited molecular signatures of brown, “brite,” and white adipose tissues.
5. Himms-Hagen J (1990) Brown adipose tissue thermogenesis: interdisciplinary studies. Faseb j 4:2890-8.
6. Nedergaard J, Golozoubova V, Matthias A, Asadi A, Jacobsson A and Cannon B (2001) UCP1: the only protein able to mediate adaptive non-shivering thermogenesis and metabolic inefficiency. Biochimica et Biophysica Acta (BBA) - Bioenergetics 1504:82-106. doi: http://dx.doi.org/10.1016/S0005-2728(00)00247-4
7. Saito M, Okamatsu-Ogura Y, Matsushita M, Watanabe K, Yoneshiro T, Nio-Kobayashi J, Iwanaga T, Miyagawa M, Kameya T, Nakada K, Kawai Y and Tsujisaki M (2009) High Incidence of Metabolically Active Brown Adipose Tissue in Healthy Adult Humans: Effects of Cold Exposure and Adiposity. Diabetes 58:1526-1531. doi: 10.2337/db09-0530
8. Cinti S (2011) Between brown and white: Novel aspects of adipocyte differentiation. Annals of Medicine 43:104-115. doi: 10.3109/07853890.2010.535557
9. Rosenwald M, Perdikari A, Rülicke T and Wolfrum C (2013) Bi-directional interconversion of brite and white adipocytes. Nat Cell Biol 15:659-667. doi: 10.1038/ncb2740

http://www.nature.com/ncb/journal/v15/n6/abs/ncb2740.html#supplementary-information
10. Cinti S (2009) Transdifferentiation properties of adipocytes in the adipose organ.
11. Nedergaard J and Cannon B (2013) How brown is brown fat? It depends where you look. Nat Med 19:540-541. doi: 10.1038/nm.3187
12. Zouhar P (2015) Importance of adipose tissue metabolism for whole-body

energy balance. Charles University in Prague

Faculty of Science.
13. Frayn KN (1989) Adipose tissue metabolism. Clinics in dermatology 7:48-61.

14. Saether T, Tran TN, Rootwelt H, Grav HJ, Christophersen BO and Haugen TB (2007) Essential fatty acid deficiency induces fatty acid desaturase expression in rat epididymis, but not in testis. Reproduction 133:467-77. doi: 10.1530/rep-06-00294
15. Forest C, Tordjman J, Glorian M, Duplus E, Chauvet G, Quette J, Beale E and Antoine B (2003) Fatty acid recycling in adipocytes: a role for glyceroneogenesis and phosphoenolpyruvate carboxykinase. Biochemical Society Transactions 31:1125-1129.
16. ANDERSSON U, Houstek J and CANNON B (1997) ATP synthase subunit c expression: physiological regulation of the P1 and P2 genes. Biochem. J 323:379-385.
17. Nicholls DG, Bernson VS and Heaton GM (1978) The identification of the component in the inner membrane of brown adipose tissue mitochondria responsible for regulating energy dissipation. Effectors of Thermogenesis, Springer, pp. 89-93
18. CANNON B and NEDERGAARD J (2004) Brown Adipose Tissue: Function and Physiological Significance.
19. Carneheim C, Nedergaard J and Cannon B (1984) Beta-adrenergic stimulation of lipoprotein lipase in rat brown adipose tissue during acclimation to cold. American Journal of Physiology-Endocrinology And Metabolism 246:E327-E333.
20. AGARWAL RCP SPECTROSCOPY OF HEAVY WATER & ITS EFFECT ON ENVIRONMENT.
21. Delgado TC, Pinheiro D, Caldeira M, Castro M, Geraldes C, López-Larrubia P, Cerdan S and Jones J (2009) Sources of hepatic triglyceride accumulation during high-fat feeding in the healthy rat. NMR in biomedicine 22:310-317.
22. Hermann A (1999) Determination of site-specific D/H isotope ratios of glycerol from different sources by 2H-NMR spectroscopy. Zeitschrift für Lebensmitteluntersuchung und-Forschung A 208:194-197.
23. Chen JL, Peacock E, Samady W, Turner SM, Neese RA, Hellerstein MK and Murphy EJ (2005) Physiologic and pharmacologic factors influencing glyceroneogenic contribution to triacylglyceride glycerol measured by mass isotopomer distribution analysis. Journal of Biological Chemistry 280:25396-25402.
24. Folch J, Lees M and Sloane-Stanley G (1957) A simple method for the isolation and purification of total lipids from animal tissues. J biol chem 226:497-509.
25. Christie WW (1993) Preparation of ester derivatives of fatty acids for chromatographic analysis. Advances in lipid methodology 2:e111.
26. Jones JG, Merritt M and Malloy C (2001) Quantifying tracer levels of 2H2O enrichment from microliter amounts of plasma and urine by 2H NMR. Magnetic resonance in medicine 45:156-158.

Appendix

Other Figures

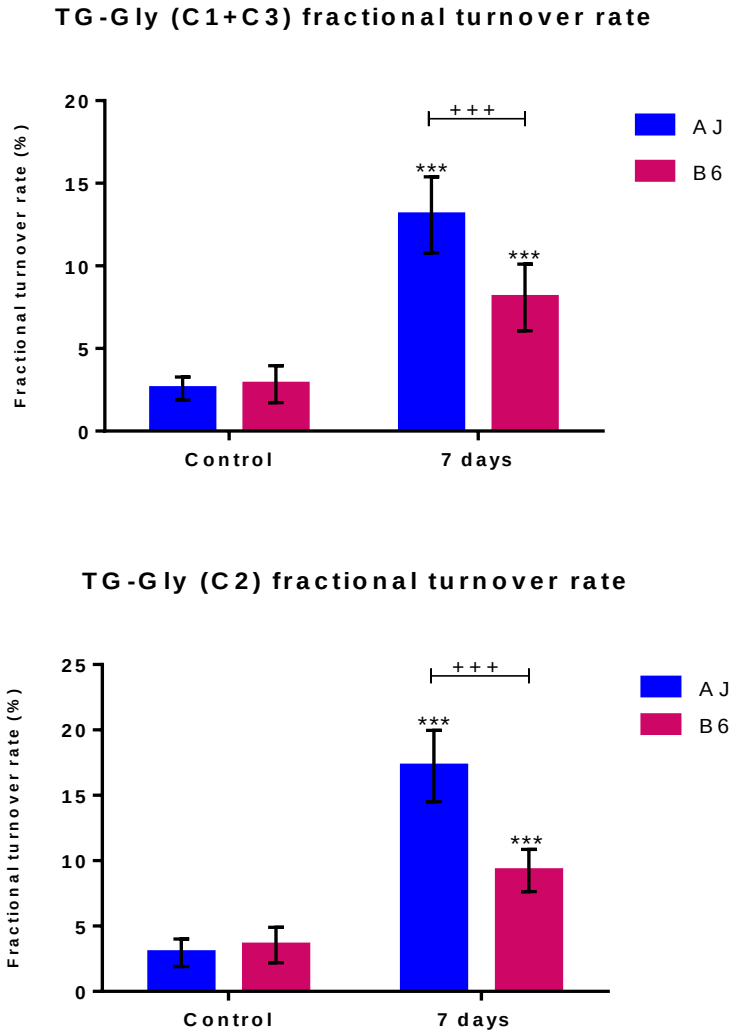

Figure A1 - Fractional turnover rates for both C1+3 and C2 of glycerol moiety corresponding to the transesterification of the first set of samples.

**** Mean values were significantly different from those of control animals (P<0.001). +++ Mean values were significantly different between the animals of 7 days groups. (P < 0,001).*

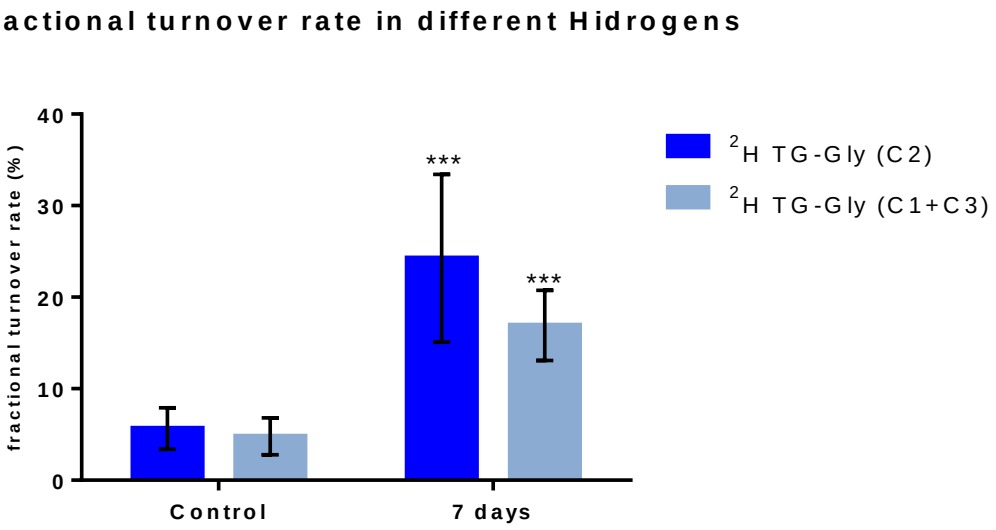

Figure A2 – Fractional synthetic rates for both C1+3 and C2 of glycerol moiety for the second set of samples where we only analysed AJ mice.

**** Mean values were significantly different from those of control animals (P<0.001).*